AD-A052 036 AEROSPACE CORP EL SEGUNDO CALIF CHEMISTRY AND PHYSICS LAB F/G 7/4
THE EFFECT OF VIBRATIONAL EXCITATION ON THE REACTION OF O(3P) W--ETC(U)
FEB 78 G C LIGHT F04701-77-C-0078

UNCLASSIFIED TR-0078(3970-40)-1 SAMSO-TR-78-49 NL

| OF |
AD
A052 036

END
DATE
FILMED
5-78
DDC

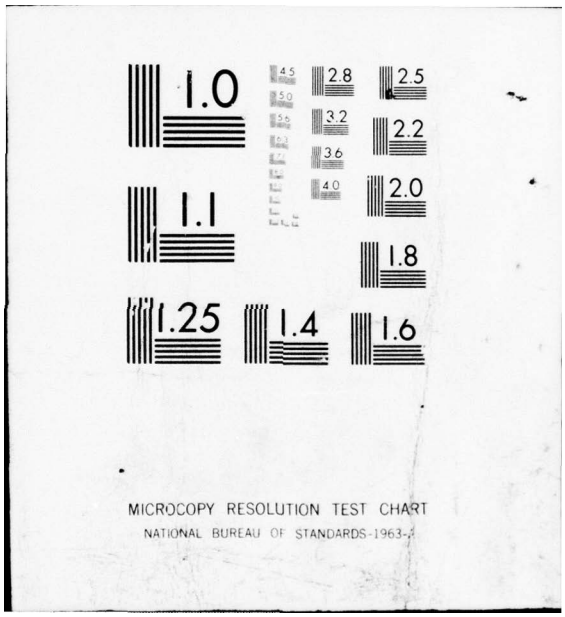
1.0
1.1
1.25
1.4
1.6
1.8
2.0
2.2
2.5
2.8
3.2
3.6
4.0
4.5
5.0
5.6
MICROCOPY RESOLUTION TEST CHART
NATIONAL BUREAU OF STANDARDS-1963-A

AD A052036

REPORT SAMSO-TR-78-49

(2) 2

# The Effect of Vibrational Excitation on the Reaction of $O(^3P)$ with $H_2$ and the Distribution of Vibrational Energy in the Product OH

AD NO. DDC FILE COPY

G. C. LIGHT
Chemistry and Physics Laboratory
The Ivan A. Getting Laboratories
The Aerospace Corporation
El Segundo, Calif. 90245

DDC RECEIVED MAR 31 1978 F

14 February 1978

Interim Report

APPROVED FOR PUBLIC RELEASE;
DISTRIBUTION UNLIMITED

Prepared for
SPACE AND MISSILE SYSTEMS ORGANIZATION
AIR FORCE SYSTEMS COMMAND
Los Angeles Air Force Station
P.O. Box 92960, Worldway Postal Center
Los Angeles, Calif. 90009

This interim report was submitted by The Aerospace Corporation, El Segundo, CA 90245, under Contract No. F04701-77-C-0078 with the Space and Missile Systems Organization, Deputy for Advanced Space Programs, P.O. Box 92960, Worldway Postal Center, Los Angeles, CA 90009. It was reviewed and approved for The Aerospace Corporation by S. Siegel, Director, Chemistry and Physics Laboratory. Lieutenant A. G. Fernandez, SAMSO/YCPT, was the project officer for Advanced Space Programs.

This report has been reviewed by the Information Office (OI) and is releasable to the National Technical Information Service (NTIS). At NTIS, it will be available to the general public, including foreign nations.

This technical report has been reviewed and is approved for publication. Publication of this report does not constitute Air Force approval of the report's findings or conclusions. It is published only for the exchange and stimulation of ideas.

Arturo G. Fernandez, Lt, USAF
Project Officer

Robert W. Lindemuth
Robert W. Lindemuth, Lt Col, USAF
Chief, Technology Plans Division

FOR THE COMMANDER

LEONARD E. BALTZELL, Col, USAF
Asst. Deputy for Advanced Space Programs

UNCLASSIFIED

SECURITY CLASSIFICATION OF THIS PAGE (When Data Entered)

| REPORT DOCUMENTATION PAGE | READ INSTRUCTIONS BEFORE COMPLETING FORM |
|---|---|
| 1. REPORT NUMBER: SAMSO-TR-78-49 | 2. GOVT ACCESSION NO. |
| 3. RECIPIENT'S CATALOG NUMBER | |
| 4. TITLE (and Subtitle): THE EFFECT OF VIBRATIONAL EXCITATION ON THE REACTION OF $O(^3P)$ WITH $H_2$ AND THE DISTRIBUTION OF VIBRATIONAL ENERGY IN THE PRODUCT OH. | 5. TYPE OF REPORT & PERIOD COVERED: Interim rept. |
| 6. PERFORMING ORG. REPORT NUMBER: TR-0078(3970-40)-1 | |
| 7. AUTHOR(s): Glenn C. Light | 8. CONTRACT OR GRANT NUMBER(s): F04701-77-C-0078 |
| 9. PERFORMING ORGANIZATION NAME AND ADDRESS: The Aerospace Corporation, El Segundo, Calif. 90245 | 10. PROGRAM ELEMENT, PROJECT, TASK AREA & WORK UNIT NUMBERS |
| 11. CONTROLLING OFFICE NAME AND ADDRESS: Space and Missile Systems Organization, Air Force Systems Command, Los Angeles, Calif. 90009 | 12. REPORT DATE: 14 February 1978<br>13. NUMBER OF PAGES: 56 (61 P.) |
| 14. MONITORING AGENCY NAME & ADDRESS (if different from Controlling Office) | 15. SECURITY CLASS. (of this report): Unclassified<br>15a. DECLASSIFICATION/DOWNGRADING SCHEDULE |

16. DISTRIBUTION STATEMENT (of this Report)

Approved for public release; distribution unlimited.

17. DISTRIBUTION STATEMENT (of the abstract entered in Block 20, if different from Report)

DDC RECEIVED MAR 31 1978 F

18. SUPPLEMENTARY NOTES

19. KEY WORDS (Continue on reverse side if necessary and identify by block number)

Reaction Rate
Vibrational Enhancement
Atomic Oxygen
Molecular Hydrogen
Product Vibrational Energy
Hydroxyl Molecule
Laser Induced Fluorescence
Experimental Data

20. ABSTRACT (Continue on reverse side if necessary and identify by block number)

The overall rate constant and the product branching rate constants have been measured for the first time for the reaction

$$O(^3P) + H_2(v = 1) \xrightarrow{k_{2a}} OH(v = 1) + H$$
$$O(^3P) + H_2(v = 1) \xrightarrow{k_{2b}} OH(v = 0) + H$$

next page

DD FORM 1473 (FACSIMILE)

UNCLASSIFIED

SECURITY CLASSIFICATION OF THIS PAGE (When Data Entered)

409 383

JOB

19. KEY WORDS (Continued)

20. ABSTRACT (Continued)

where $k_2 = k_{2a} + k_{2b}$. The measurements were made in a flow tube apparatus at T = 302 ± 2 K at a total pressure of 3 Torr. $O(^3P)$ was produced by the titration of active nitrogen with NO. $H_2(v = 1)$ was produced by a heated tungsten filament, and its concentration was determined from VUV absorption measurements in the Lyman band system of $H_2$. Absolute concentrations of OH(v = 0) and OH(v = 1) were deduced from laser induced fluorescence in OH in a calibrated fluorescence system. The rates and uncertainties are:

$$k_2 = \left(1.0^{+0.9}_{-0.6}\right) \times 10^{-14} \text{ cc/molecule-sec}$$

$$k_{2a} = \left(1.0^{+0.4}_{-0.6}\right) \times 10^{-14} \text{ cc/molecule-sec}$$

$$k_{2b} \leq 4.7 \times 10^{-15} \text{ cc/molecule-sec}$$

The reported value for $k_2$ represents an increase owing to vibrational excitation in hydrogen by a factor of $\approx 2.6 \times 10^3$ over the fully ground state reaction rate constant. Measurements of the fully ground state reaction rate constant and recent theoretical treatments of the $O + H_2$ reaction are discussed in relation to these results.

## PREFACE

The author thanks Prof. Graham Glass for a preprint and would like to acknowledge many stimulating discussions with Prof. J. V. V. Kasper, Dr. L. R. Martin, and Dr. R. R. Herm during the course of investigation. The expert help of James H. Matsumoto in obtaining the data is greatly appreciated. The interest and advice of Dr. R. J. McNeal is gratefully acknowledged.

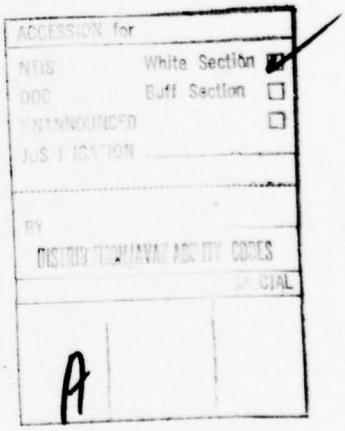

CONTENTS


PREFACE . . . . . 1

I. INTRODUCTION . . . . . 7

II. EXPERIMENTAL . . . . . 9

a. Apparatus . . . . . 9

b. Procedure and Calibration . . . . . 14

III. RESULTS AND ANALYSIS . . . . . 29

a. $\xi \gg 1$ . . . . . 33

b. $\xi \approx 1$ . . . . . 37

c. $\xi \ll 1$ . . . . . 38

d. Final Rate Constants . . . . . 38

e. Sensitivity Analysis . . . . . 39

IV. DISCUSSION . . . . . 47

REFERENCES . . . . . 55

APPENDIXES

A. REACTIONS USED FOR THE CALCULATION OF SPECIES CONCENTRATIONS IN THE N + NO SYSTEM . . . . . 59

B. REACTIONS USED FOR COMPUTER CALCULATIONS IN THE O + $H_2$ SYSTEM . . . . . 61


Preceding Page BLANK

## FIGURES


1. Conceptual Drawing of the Apparatus . . . . . 10

2. Calculated Species Concentrations As a Function of NO Flow Rate for the Reactions Listed in Appendix A . . . . . 15

3. The Dependence of $NO_2$ Concentration on the Flow Rate of NO . . . . . 17

4. Experimental Data for Fluorescence Decay of $OH(A^2\Sigma^+)$ . . . . . 22

5. Experimental Data That Show Nonlinear Fluorescence Behavior, Owing to Partial Optical Saturation . . . . . 25

6. An Excitation Fluorescence Spectrum of the (0-0) Band in OH . . . . . 30

7. Data for the Density of OH(v = 0, 1) As a Function of the Flow Rate of NO for Constant N-Atom Flow Rate . . . . . 31

8. Comparison of the Computer-Calculated Densities of OH(v = 0, 1) With the Experimental Data Shown in Fig. 7 . . . . . 40

9. A Summary of Present Knowledge of the Rate Constant for Reaction (2) . . . . . 50

10. The Rate Constant for Reaction (1) in the High-Temperature Region . . . . . 52


## TABLES


I. Electronic Quenching Rates of $OH(A^2\Sigma^+, v' = 0)$ . . . . . 23

II. Experimental Data Used To Find $(k_{2a}/k_{8a})$ from Expression (g) . . . . . 36


Preceding Page BLANK

# I. INTRODUCTION

The reaction of $O(^3P)$ with $H_2$ has been the subject of many investigations in the last twenty years.[1-4] A review of all of the measurements through June 1971 is presented in Ref. 5. In the temperature range from 400°K to 2000°K there is general agreement as to the value of the rate constant. There have been no reported measurements of the rate of this reaction for vibrationally excited hydrogen. The fully ground state reaction

$$O(^3P) + H_2(v = 0) \longrightarrow OH(v = 0) + H \qquad (1)$$

is endothermic by about 2.0 kcal/mole and has an activation energy of about 8.9 kcal/mole.[5] When the $H_2$ has one quantum of vibrational energy, reaction (2a)

$$O(^3P) + H_2(v = 1) \longrightarrow OH(v = 1) + H \qquad (2a)$$

is barely endothermic ($\approx$ 0.3 kcal/mole) and reaction (2b)

$$O(^3P) + H_2(v = 1) \longrightarrow OH(v = 0) + H \qquad (2b)$$

is exothermic by 9.9 kcal/mole. Thus, it is seen that if vibrational energy in $H_2$ is effective in overcoming the activation energy of reaction (1), the ratio $k_2/k_1$, where $k_2 = k_{2a} + k_{2b}$, might be extremely large. Birely et al.[6] have reported an upper limit to the value of $k_2$ such that $k_2/k_1 \leq 3.4 \times 10^4$ at T = 300°K. This means that at most the fraction $\alpha = 0.52$ of the $H_2$ vibrational energy is effective in reducing the activation energy.[7] In addition, there have been two reports of theoretical

Preceding Page Blank

treatments of this reaction.[8,9] Johnson and Winter[8] report an Arrhenius expression for $k_2$,

$$k_2 = 4.65T \times 10^{-14} \exp(-1868/T) \text{ cc/molecule-sec.},$$

which is lower than the upper bound established by Birely et al. at $T = 300^{\circ}K$.

Interest in the dependence of elementary reaction rate constants on particular quantum states of reactants and products has grown enormously in the past two decades. These data are important in characterizing the detailed mechanism and potential energy hypersurface for a reaction, and in more practical application to such areas as molecular lasers, laser-initiated chemistry, laser isotope separation and chemical processes occurring under a variety of other nonequilibrium situations. Molecular beam, chemiluminescence and chemical laser studies have led to the characterization of energy partitioning in a variety of elementary reactions. However, the effect of reactant vibrational energy is not well characterized and measurements which are differential with respect to both reactant and product quantum states are very rare.

This paper reports for the first time a measurement of the rate of the reaction

$$O(^3P) + H_2(v = 1) \xrightarrow{k_{2a}} OH(v = 1) + H. \qquad (2a)$$

Also reported is an upper limit to the value of $k_{2b}$, where

$$O(^3P) + H_2(v = 1) \xrightarrow{k_{2b}} OH(v = 0) + H. \qquad (2b)$$

## II. EXPERIMENTAL

### a. Apparatus

The measurements were conducted at 302 ± 2°K in the flow tube apparatus shown schematically in Fig. 1. Atomic oxygen, $O(^3P)$, was generated by the rapid reaction $N + NO \longrightarrow N_2 + O$, for which the N-atoms were provided by a microwave discharge in pure $N_2$. Nitric oxide was admitted to the flow tube through a circular ring of small radial holes in the wall of the flow tube. Between the $N_2$ microwave discharge and the NO titration inlet there was placed a side arm for the admission of bypass $N_2$ gas. The purpose for this bypass flow is discussed later. Some 14 cm downstream from the NO titration inlet the O-atoms were allowed to mix with pure $H_2$ gas containing vibrationally excited $H_2(v = 1)$. Vibrational excitation in the hydrogen was created by passing the $H_2$ through a 1 cm diameter alumina tube containing a densely wound tungsten filament which was electrically heated. Upon exiting from this gas heater, rotational and translational modes of the $H_2$ were equilibrated with the room temperature flow tube walls before mixing with the O-atom stream. However, the VUV absorption measurements confirmed that the vibrational modes of $H_2$ equilibrate much more slowly with the walls. Hence, we have a slowly decaying $H_2(v = 1)$ density as a function of distance traveled down the flow tube. Auxiliary measurements without the O-atom source confirmed the absence of any OH production by a possible oxidation of the $H_2$ on the hot alumina surfaces. An annular cooling water jacket was provided in the flow tube walls between the bottom of the gas heater and the reactant mixing point for the purpose of ensuring a controlled wall temperature.

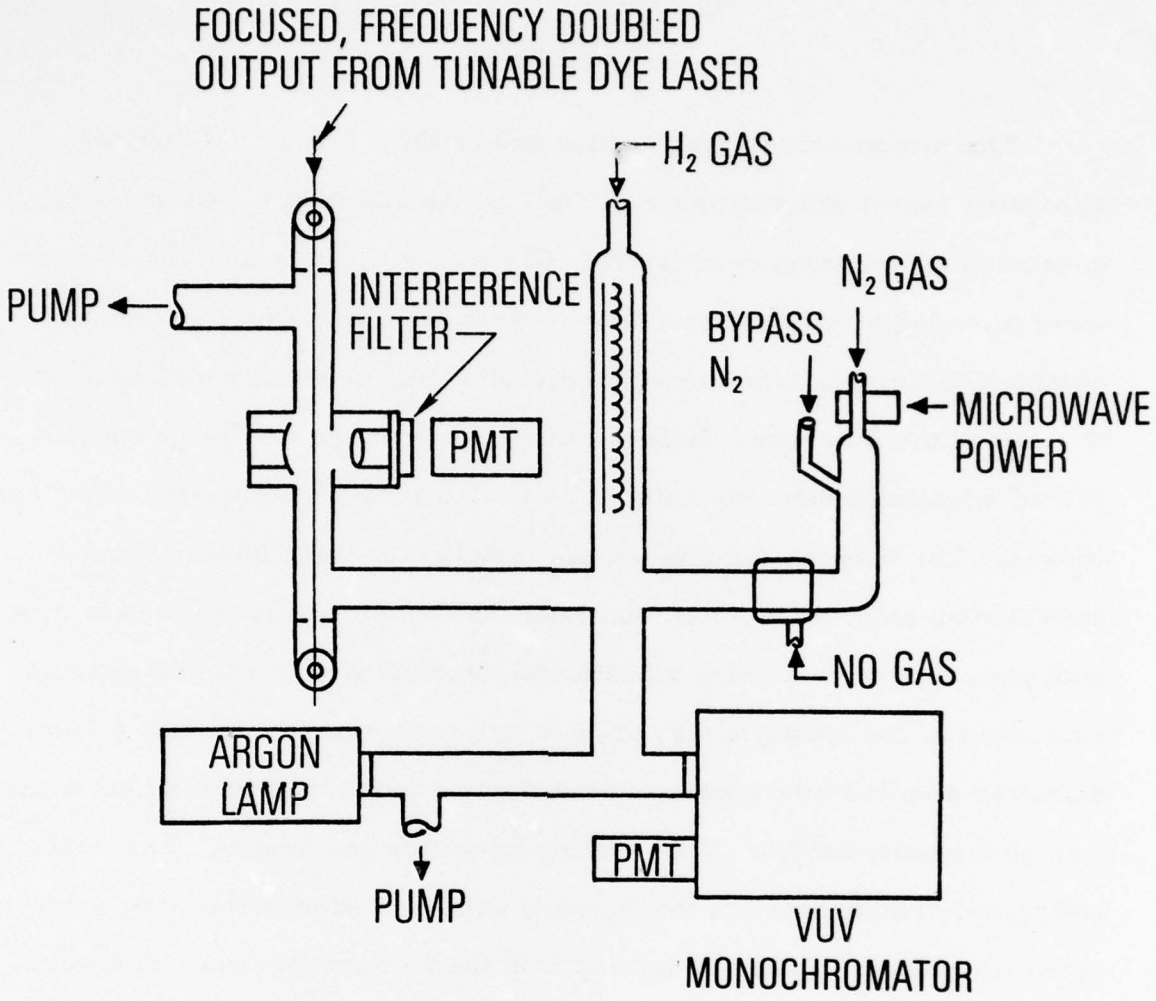


**Fig. 1. Conceptual Drawing of the Apparatus**

From the point where the O and $H_2$ reactant streams meet they could be directed into either of two portions of the flow tube. They could be convected into the VUV absorption cell where quantitative measurements of the density of $H_2(v = 0)$ and $H_2(v = 1)$ were performed. Conversely, the gas flow could be convected to a section of flow tube designed for the generation and collection of laser induced fluorescence in the product OH molecules. The OH fluorescence cell and the center of the VUV absorption cell were equidistant from the point where the reactant streams mixed. The light source for the VUV absorption measurements was a pulsed dc electrical discharge in argon. This discharge produces the argon continuum between 110 and 140 nm. This emission passes through a lithium fluoride (LiF) window into a 14-cm-long absorption path in the flow tube. It then exits from the flow tube, passes through yet another LiF window and through the entrance slit of a scanning VUV monochromator. In operation, the monochromator is scanned slowly through a particular rotation-vibration line in the Lyman band system of $H_2$. For measurements of $H_2(v = 1)$ density, absorption by the P(1), R(2) line blend of the (1, 1) band at $\lambda = 114.62$ nm was measured. The resulting absorption trace was manually integrated to yield equivalent width. The density of $H_2(v = 1)$ was then deduced from curve-of-growth calculations.[10] The accuracy of the curve-of-growth analysis was verified by absorption measurements in the (0, 0) band of this system and corresponding pressure measurements with a bourdon type pressure gauge.

For the laser induced fluorescence measurements of OH density, focused, tunable laser radiation entered the flow tube through a quartz window oriented at Brewster's angle. It then passed through some optical baffles, was directed

along the flow tube axis through more optical baffles and exited through another quartz Brewster angle window. Laser pulse energy was measured by a pyroelectric detector in the exit beam. Laser induced fluorescence was collected by a quartz lens on one side of the flow tube and by an aluminized spherical mirror diametrically opposite the lens. These two elements were arranged with an optical aperture of f/1.5. Collected radiation then passed through a broadband interference filter and directly into a photomultiplier tube (EMI 9635QB). The filter had a peak transmission of 24% at $\lambda$ = 312.5 nm, 12% at $\lambda$ = 305.5 nm and $\lambda$ = 318.0, and less than 1% for $\lambda \leq 299.5$ nm and $\lambda \geq 328.5$ nm. Hence, this filter readily passed radiation in the (0-0) and (1-1) bands of the $OH(A^2\Sigma \longrightarrow X^2\Pi)$ system. The PMT anode was terminated in a 50 ohm resistor at the input of a preamplifier (70 MHz bandpass, gain = 10). The preamp output was connected to a PAR Model 162 Dual Channel Boxcar Averager.

The excitation source was a Molectron DL-200 tunable dye laser. The laser output was frequency doubled with a 4 cm long angle tuned crystal of ADP. After frequency doubling to $\lambda$ = 308.5 nm; the typical laser pulse contained 5 to 10 x $10^{-6}$ joules of energy, was approximately 5 x $10^{-9}$ sec in duration, and 1.0 $cm^{-1}$ in spectral width. The laser was operated at a pulse rate of 25 Hz.

The flow tube was constructed of Pyrex glass, with an internal diameter of 25 mm. The average gas flow velocity was 15 m/sec. Experiments were conducted with a fixed total pressure of 3.0 Torr comprised of equal parts of $N_2$ and $H_2$. The exterior surface of the flow tube was instrumented with three thermocouples, one at the point where O and $H_2$

reactants mixed, one at the fluorescence cell and the third midway between these two. Most of the inside surface of the flow tube was coated with a halocarbon wax which has been shown[11] to be effective in controlling the heterogeneous removal rate of various atoms and radicals at the walls. No coating was applied in the region near the hot tungsten filament. In the immediate vicinity of the microwave discharge boric acid was applied to the tube walls. The acid was converted to the powdery white oxide by heating the glass from the outside with a propane torch.

The flow rates of $N_2$ and $H_2$ gases were monitored by Matheson rotameter gauges. The flow rate of nitric oxide was determined by measuring the pressure drop in a known reservoir volume. The O-atom density was deduced at the visible chemiluminescence titration end point[12] from the known NO flow rate and computer integration of a set of twelve chemical reactions. These same calculations provided the densities of several minor species which accompany the N + NO system and whose role in the overall kinetics of OH production and removal must be understood.

The gases used in the experiment all were supplied by Matheson Company with the following stated purities: $H_2$, UHP grade 99.999% min., $N_2$, UHP grade 99.999% min., and NO, C.P. grade, 99.0% min. Both the $H_2$ and $N_2$ were further purified by passing through traps filled with glass beads at 77°K and 700 Torr pressure. The nitric oxide was purified by three successive distillations between traps at 77°K and 156°K (ethanol slush).

### b. Procedure and Calibration

Fluorescence amplitude data were obtained by tuning the laser output frequency through a particular rotational line in the ($A^2\Sigma^+ \rightarrow X^2\Pi_i$) system of OH. This procedure provided a measure of the background signal and the sum of the background and fluorescence signals for each observation. The $Q_1(1)$ line was used in both the (0-0) and the (1-1) bands to collect detailed data on OH(v) density. Fluorescence radiation was collected from the (0-0) band when the v'' = 0 state was investigated and from both the (0-0) and the (1-1) bands simultaneously, when the v'' = 1 state was investigated.

The density of nitric oxide and of several other important species was conveniently varied by changing the ratio of nitric oxide inlet flow rate to N-atom flow rate. This ratio is hereafter referred to as, $\xi \equiv \Phi_{NO}/\Phi_N$, where $\Phi$ stands for flow rate in units of particles/sec. The computed dependences of the densities of O, N, NO, and $NO_2$ on $\xi$ are shown for a typical case in Fig. 2. The kinetic scheme used to compute these results is detailed in Appendix A. As a test of the ability of the computer code for numerical integration of the chemical rate equations to accurately simulate the chemistry in this experiment it was decided to measure the density of $NO_2$ produced by the N + NO system for comparison with calculated values. For this purpose calibrated laser induced fluorescence data were obtained for $NO_2$. The laser was tuned to 445.0 nm and fluorescence was observed with a photomultiplier/filter combination

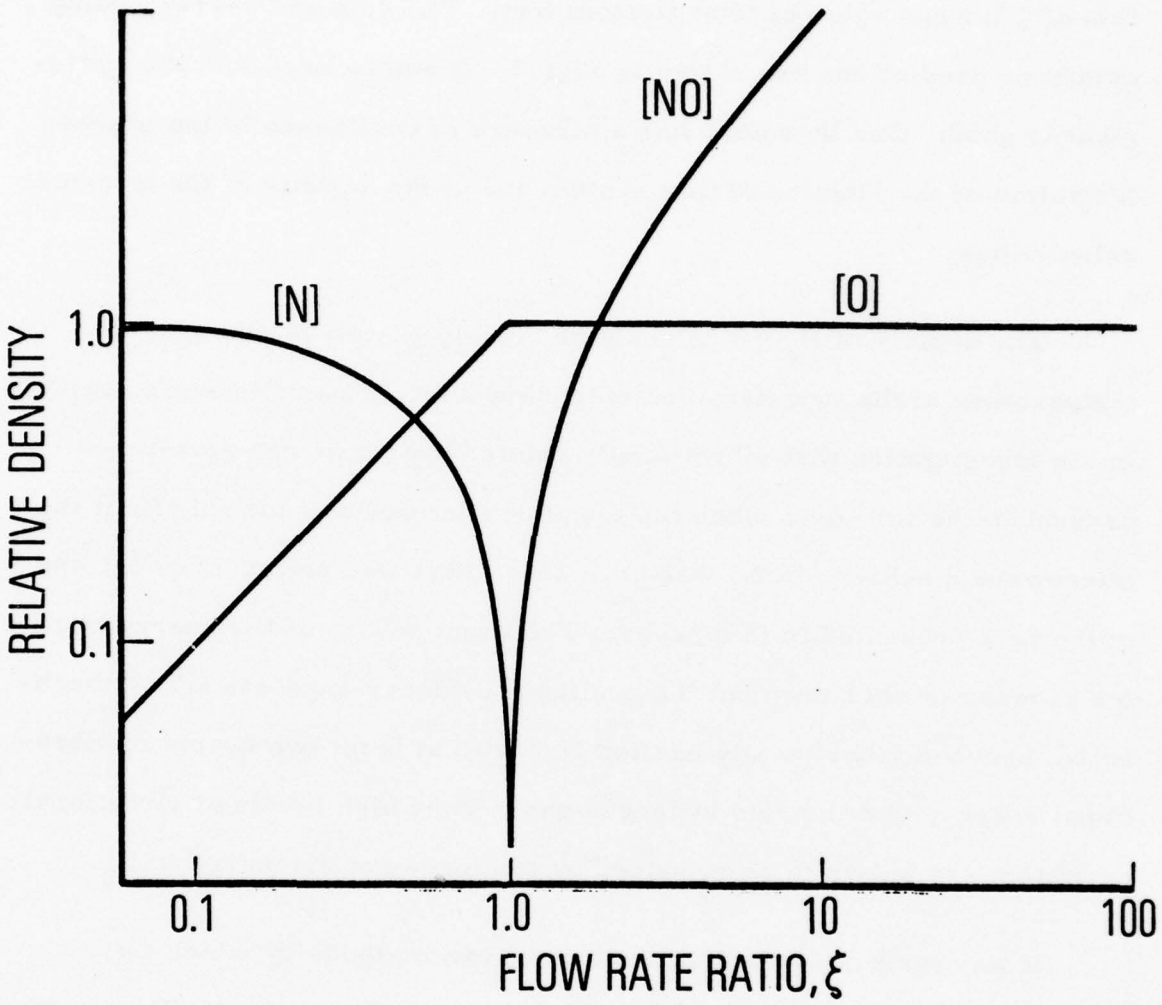


Fig. 2. Calculated Species Concentrations As a Function of NO Flow Rate for the Reactions Listed in Appendix A

for $\lambda \geq 480$ nm. Data were obtained for fluorescence intensity as a function of $\xi$ for one value of total N-atom flux. The data and corresponding computer predictions are shown in Fig. 3. It can be seen that the agreement is good. One therefore has a measure of confidence in the characterization of the kinetics of this system and in the validity of the computer calculations.

The density of $H_2(v = 1)$ could be readily varied by changing the temperature of the tungsten filament. However, it was discovered early in the investigation that vibrationally excited hydrogen was sometimes present in the flow even when the tungsten filament was turned off, if the microwave discharge in $N_2$ was on. This effect was unimportant for any of the data presented in this paper. The exact nature of the energy transfer process is not known but the available evidence suggests a V-V mechanism between vibrationally excited $N_2$, with at least two quanta of vibrational energy, and the cold hydrogen gas. Very high levels of vibrational excitation are known to be produced by a microwave discharge in $N_2$.

It was further found that there were two methods by which this energy transfer was prevented. By adding a small amount of $CO_2$ gas to the discharged $N_2$ stream before it contacted the $H_2$ flow, the generation of $H_2(v \geq 1)$ by this process was prevented. It was also verified that there was no effect on the density of $H_2(v = 1)$ if $CO_2$ was titrated into the flow in the absence of active nitrogen. The $CO_2$ evidently quenches the active nitrogen without directly affecting $H_2(v = 1)$. The second method involved

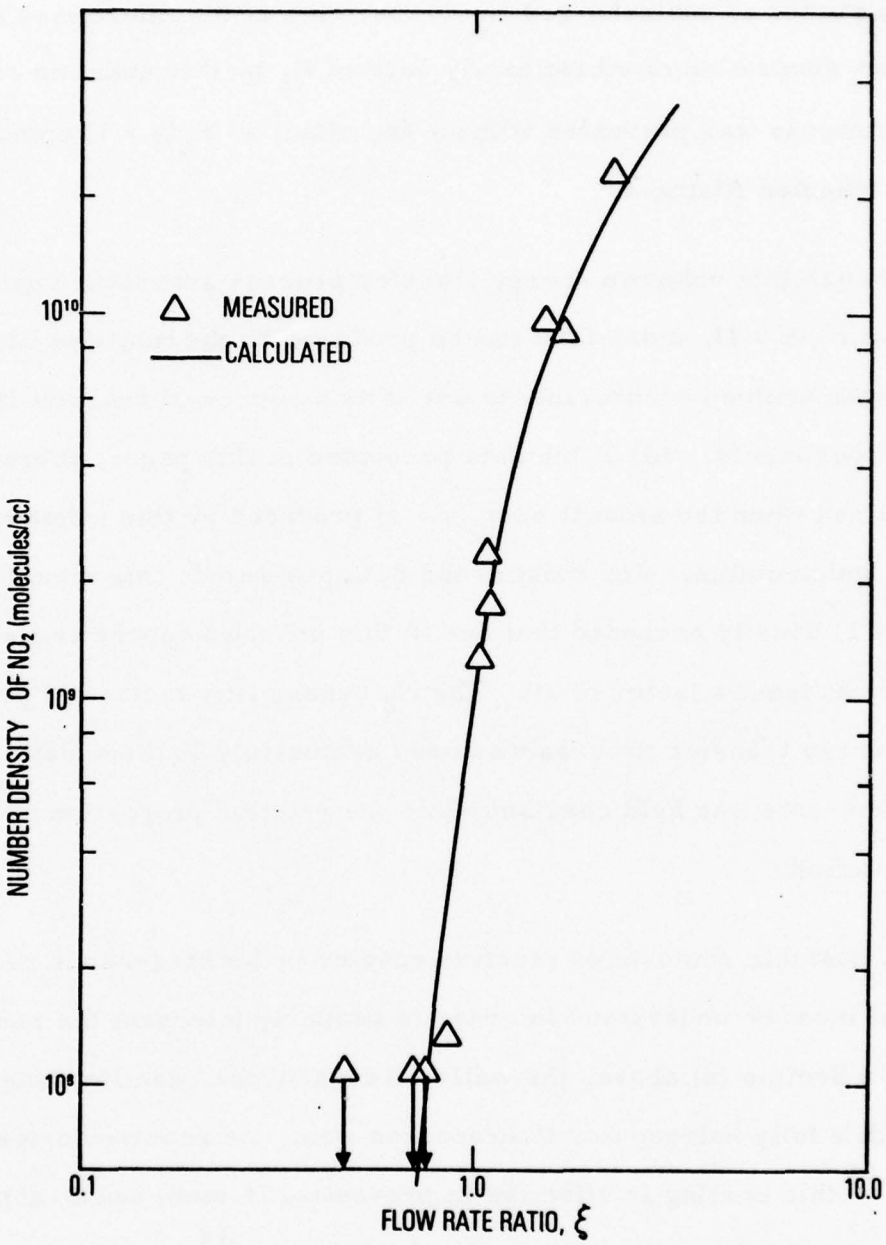


Fig. 3. The Dependence of $NO_2$ Concentration on the Flow Rate of NO. The measured $NO_2$ density was deduced from laser induced fluorescence data on $NO_2$.

adding an excess of undischarged $N_2$ downstream of the microwave discharge; the generation of vibrationally excited $H_2$ by this unknown energy transfer process was prevented without any effect on $H_2(v = 1)$ coming from the tungsten filament.

Although this unknown energy transfer process generates copious amounts of $H_2(v = 1)$, more than can be produced by the tungsten filament alone, it was deemed unadvisable to use it as a source of reactant in the present experiments. All of the data presented in this paper, therefore, were obtained when the amount of $H_2(v = 1)$ produced by this unknown process was undetectable. For most of the data presented, this meant that the $H_2(v = 1)$ density exceeded that due to this unknown energy transfer process by at least a factor of 30. The $N_2$ bypass flow method of preventing this energy transfer process was used exclusively in these data. The total $N_2$ flow rate was held constant while the relative proportion of bypass flow was varied.

The possible removal of reactive species by heterogeneous reactions at the wall must be understood in order to properly interpret the results. As noted in Section (a) above, the walls throughout the reaction zone are coated with a fully halogenated fluorocarbon wax. As reported originally by Glass,[11] this coating is effective in preventing H-atom and O-atom recombination on the walls. Glass also has reported[13] a wall removal rate expressed as a first order rate constant of $k_w = -30\ sec^{-1}$ for OH and a vibrational relaxation rate for $OH(v = 1)$ of $k_w \leq -80\ sec^{-1}$ when such a

wax is used to coat the walls. These rates are sufficiently slow that the removal of these species is dominated by homogeneous gas phase reactions under all conditions encountered in this experiment. For $H_2(v = 1)$, Birely et al.[6] reported $k_w$ in the range -62 to -91 $sec^{-1}$ for an uncoated Pyrex wall. We have measured an average value of $k_w = -46$ $sec^{-1}$ for $H_2(v = 1)$ deactivation on a halocarbon wax coated wall. This value was derived from measurements of the density of $H_2(v = 1)$ as a function of the exposed length of coated glass tube. Because $H_2(v = 1)$ does not react rapidly with any species present in these experiments, this wall deactivation has a minor effect on the OH(v) kinetics. As will be documented later, the homogeneous gas phase removal processes for both OH(0) and OH(1) are sc fast that it is of primary importance to know the density of $H_2(v = 1)$ only at the point where measurements of OH(v) densities are made and of only secondary importance to know the time history of $H_2(v = 1)$ density along the tube.

Wavelength calibration of the exciting laser radiation was accomplished by obtaining an excitation spectrum for OH laser induced fluorescence on a propane flame at atmospheric pressure. Fluorescence was detected from more than one hundred separate lines in the (0-0) and (1-1) bands of OH with a standard deviation of 0.07 A between measured wavelength and wavelengths for OH taken from Dieke and Crosswhite.[14]

As will be documented later, the loss processes for both $OH(v = 0)$ and $OH(v = 1)$ are sufficiently rapid and the depletion of reactants is

sufficiently slow that a steady state analysis of the data is required wherein it is necessary to obtain the absolute density of OH(v) in order to obtain rate constants.

The reaction $H + NO_2 \longrightarrow OH(v) + NO$ was used as a quantifiable source of OH(v = 0) in order to calibrate the fluorescence amplitude. Details of this procedure with corroborating experimental evidence and a discussion of the underlying chemical kinetics will be given elsewhere.[15] Briefly, the $H + NO_2$ reaction is relied on only as a source of OH(v = 0). The calibration for OH(v = 1) comes from supplementary measurements in the $O + H_2$ system. The justification for using $H + NO_2$ rests partly on the recently published values[13] for the rate of physical deactivation of OH(v) by H and by NO. These rates are sufficiently rapid that the resultant density of OH(v = 0) after about 10 msec of reaction time, is reasonably well defined irrespective of the present uncertainty in the branching ratios for producing different OH vibrational states.[13, 16, 17] It is true that the magnitude of the quenching rates of OH(v) by H and by NO as reported by Glass[13] are dependent on a knowledge of just these branching ratios. However, the present uncertainty in these branching ratio values and the corresponding uncertainties in the vibrational quenching rates do not appreciably influence the calculated OH(v = 0) densities.

The absolute sensitivity for detection of OH(v = 0) in the $H + NO_2$ system was obtained for laser excitation on the $Q_1(1)$ line of the (0, 0) band. In order to determine the calibration in the $O + H_2$ system a correction

must be made for differences in electronic quenching of $OH(A^2\Sigma^+, v' = 0)$ between the two gas systems. The only significant difference is in the pressure of $H_2$ which is 1.5 Torr in the case of $O + H_2$ and is appreciably lower in the case of the $H + NO_2$ data. Measurements were obtained for the quenching coefficient in $N_2$, and in $H_2$ and an upper limit was obtained in argon diluent. The fluorescence decay rate was determined by slowly scanning a narrow gate (12 nsec aperture duration) across the fluorescence signal using the Boxcar Averager. An example of the fluorescence decay data obtained is shown in Fig. 4. Data of this type were obtained at a number of different values of quenching gas pressure. The deduced quenching coefficients are shown in Table I along with some recently published values.[18] The agreement is seen to be remarkably good.

The relevant expression for the density of OH(v = 0) is:

$$[OH(v = 0)] = K_0 \left( \frac{V_s}{Q_l f_s} \right)_{(0-0)}, \qquad (a)$$

where

$K_0$ is the calibration coefficient for OH(v = 0), valid for this system only.

$V_s$ is the peak signal voltage as the laser is scanned through the $Q_1(1)$ line.

$Q_l$ is the laser pulse energy.

$f_s$ is a dimensionless factor which corrects for nonlinear optical absorption, i.e., partial optical saturation.

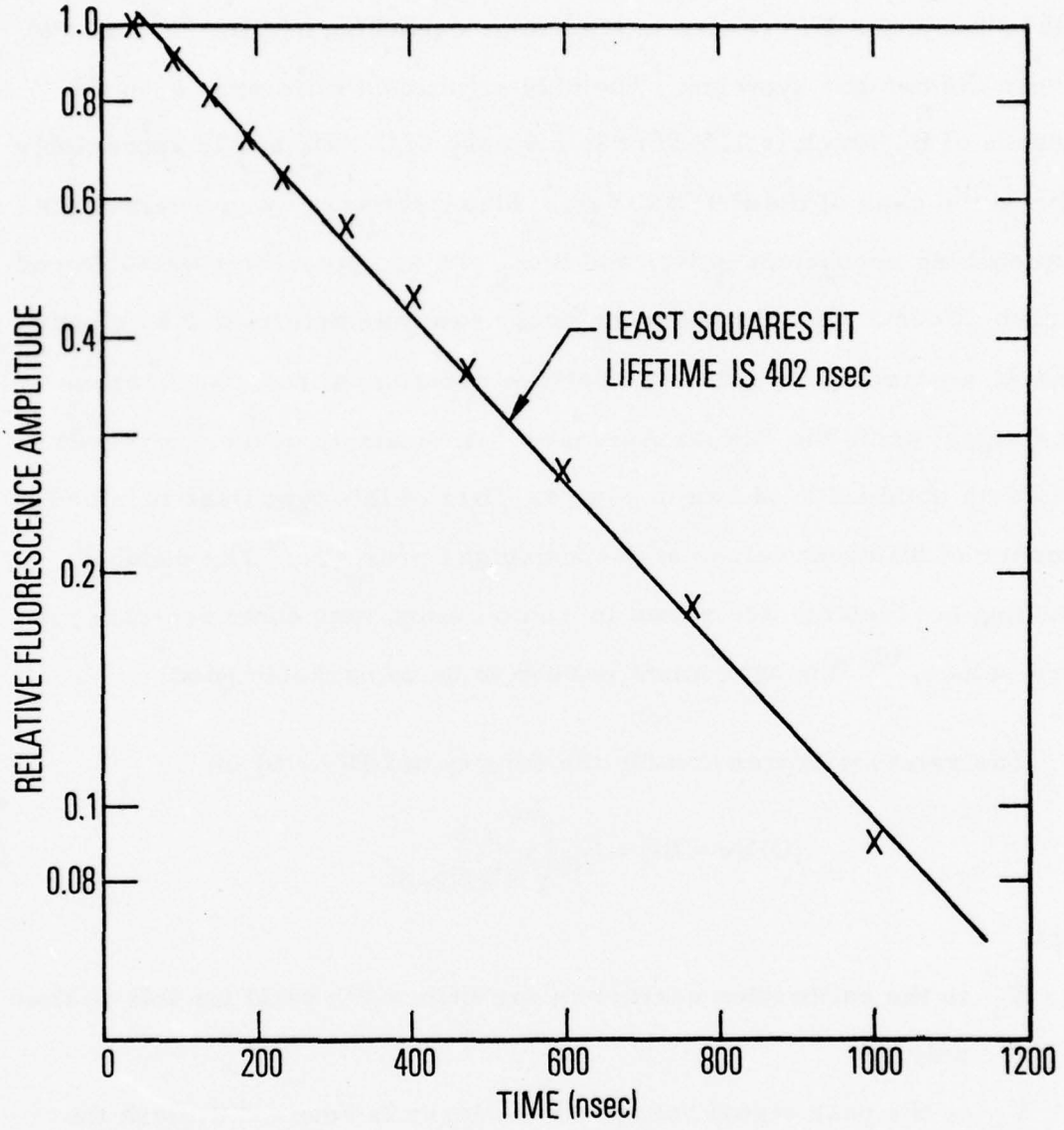


Fig. 4. Experimental Data for Fluorescence Decay of $OH(A^2\Sigma^+)$. The conditions for these data were $P_{H_2} \approx 0.0$, $P_{Ar} = 1.50$ Torr, $P_{N_2} = 1.5$ Torr. The least-squares fit to the data yields a lifetime of $\tau = 402 \times 10^{-9}$ sec.

Table I. Electronic Quenching Rates of $OH(A^2\Sigma^+, v' = 0)$

(in cc/molecule-sec)

| Quenchant | $k_q$ (Ref. 18) | $k_q$ (This work) |
|---|---|---|
| $H_2$ | $1.3 \times 10^{-10}$ | $1.35(\pm .14) \times 10^{-10}$ |
| $N_2$ | $1.95 \times 10^{-11}$ | $1.99(\pm .49) \times 10^{-11}$ |
| Ar | $5 \times 10^{-13}$ | $< 1.5 \times 10^{-12}$ |

Nonlinear optical absorption[19-22] was observed in the OH fluorescence data collected in this experiment. Data which clearly show the transition from linear to nonlinear behavior are shown in Fig. 5. These were obtained by placing filters of successively greater optical density in the laser beam before it entered the fluorescence cell. The linearity of the photomultiplier detection system was established in separate experiments.

The functional form to be expected for the dependence of fluorescence on incident laser beam energy would be difficult to calculate here. There is a wide distribution of power densities represented in the field of view of the photomultiplier detector because the laser beam is focused in the center of this field. The observed nonlinearity is effectively the result of the volume integral of the fluorescence over the irradiated region as modified by the collection efficiency of the optics for each point in the field. In addition, it may be necessary to account for power broadening of the absorption line as done by Killinger et al.[23] Our approach is strictly empirical. The factor $f_s$ in Eq. (a) is the ratio of the observed fluorescence signal to what the signal would have been if the nonlinearity had not set in. It was determined from data such as are shown in Fig. 5. Similar data were obtained for every transition used for quantitative fluorescence measurements.

A somewhat different procedure had to be used to obtain a calibration for OH(v = 1) since quantifiable sources are not readily available. With a known density of $OH(X^2\Pi_i, v'' = 0, N'' = 1, J'' = 3/2)$, i.e., the

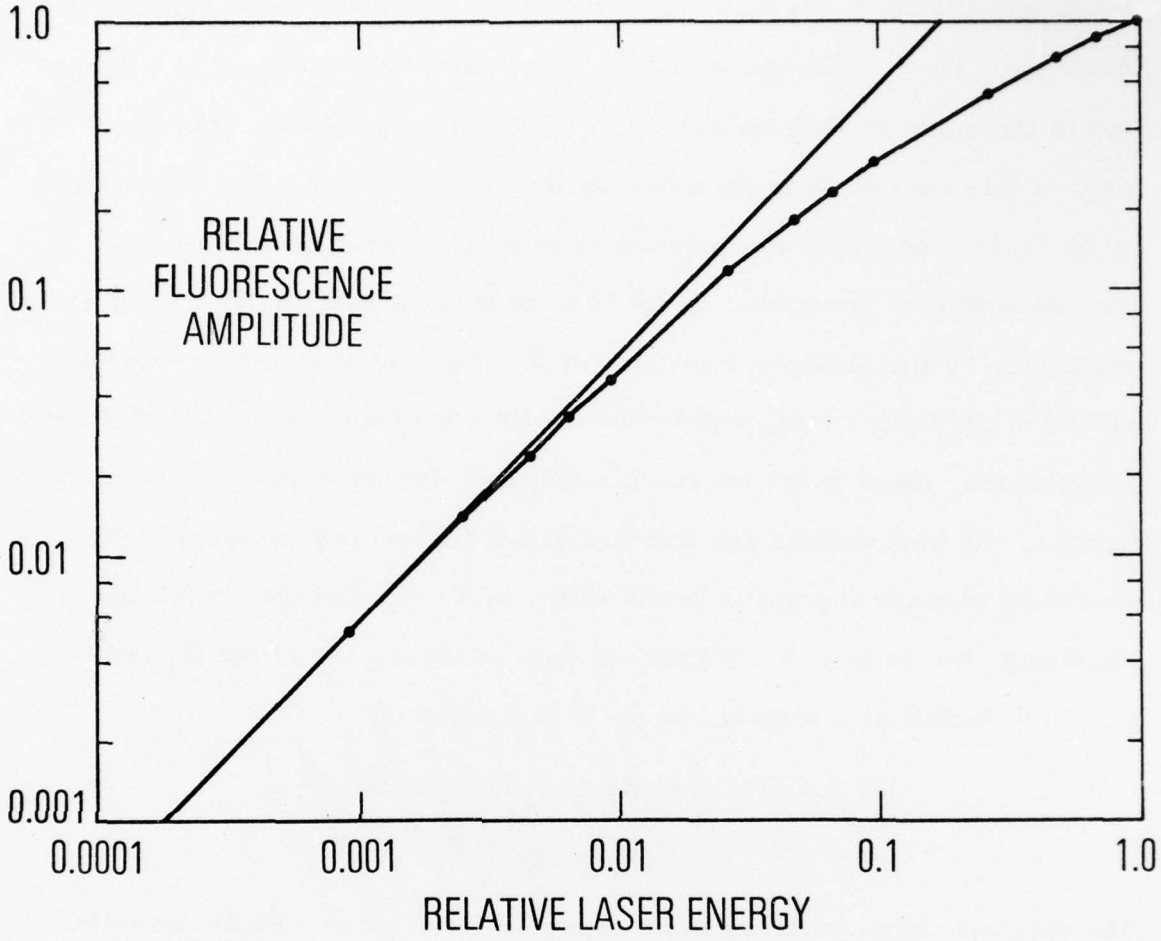


Fig. 5. Experimental Data That Show Nonlinear Fluorescence Behavior, Owing to Partial Optical Saturation. The laser excitation was on the $Q_1(1)$ line of the (0, 0) band of OH. The laser beam energy was 5.4 μJ at a value of 1.0 on the relative energy scale.

lower level of the $Q_1(1)$ transition, the laser was tuned to the $Q_1(1)$ line in the ($v' = 1$, $v'' = 0$) band at 281.915 nm. The lower level of this transition is the same as that for the $Q_1(1)$ line in the (0, 0) band. The upper level of this transition is the same as the upper level in a $Q_1(1)$ transition in the (1, 1) band. The fluorescence intensity observed for (1, 0) band excitation differs from what would have been observed for (1, 1) band excitation only by the differing densities of the lower states, i.e., the ratio $[OH(v'' = 1)]/[OH(v'' = 0)]$, and by the known transition probabilities, A, and wavelengths, laser pulse energies, and nonlinear absorption correction factors. No corrections are necessary for differences in fluorescence spectrum because the upper levels of the laser excitations are identical. Formally, the ratio of the signal voltages at the center of the $Q_1(1)$ lines for (1-0) excitation compared to (1-1) excitation is:

$$\frac{(V_s)_{1-1}}{(V_s)_{1-0}} = \frac{(\lambda^3 A f_s Q_\ell)_{(1-1)}}{(\lambda^3 A f_s Q_\ell)_{(1-0)}} \left( \frac{[OH(v'' = 1)]}{[OH(v'' = 0)]} \right) \qquad \text{(b)}$$

The ratio of signal voltages to be expected for (1-0) and (0-0) excitation differs because the upper level of the laser induced OH transition differs. This ratio must account then for electronic quenching, V-V transfer in the $A^2\Sigma^+$ state,[24] rotational redistribution in $v' = 1$ and $v' = 0$, and the wavelength dependent filter transmission function. For our purposes, it was easier to measure the integrated effect of these differences and apply an empirically determined correction factor, $C_F$, where

$$C_F = \frac{(Q_\ell f_s \lambda^3 A)_{(0-0)}}{(Q_\ell f_s \lambda^3 A)_{(1-0)}} \left( \frac{V_{1-0}}{V_{0-0}} \right) \qquad \text{(c)}$$

Combining expressions (a), (b) and (c) leads to a numerical value for $K_1$, for use in the following expression

$$[OH(v'' = 1)] = K_1\left(\frac{V_s}{f_s Q_\ell}\right)_{(1-1)}, \text{ molecules/cc.} \qquad \text{(d)}$$

The numerical value of $K_1$ is peculiar to our apparatus but includes the following ratios of transition probabilities. $A_{(1-1)}/A_{(1-0)} = 1.58$, from Crosley and Lengel,[25] and $A_{(1-0)}/A_{(0-0)} = 0.30$, from Rouse and Engleman.[26]

## III. RESULTS AND ANALYSIS

A typical OH excitation fluorescence spectrum obtained in this experiment is shown in Fig. 6. This was obtained by simultaneously tuning the laser and frequency doubling crystal over the wavelength interval shown and recording the output of the Boxcar Averager. The $Q_1(1)$ line was used for quantitative work because it is a strong transition with a large fractional population in the lower level and it is well isolated from possibly interfering lines.

Data for the dependence of OH(v = 0, 1) density on the flow rate of NO are shown in Fig. 7. The rate constants reported in this paper are derived from these and similar data. These were obtained for constant inlet N-atom density and $H_2(v'' = 1)$ density. These data were obtained by changing the NO gas flow rate for chronologically sequential data points in a random way, so as to minimize the effect of systematic trends.

The kinetics of the $O + H_2$ system were modeled using a computer code[27] which integrates the chemical rate equations for a constant area streamtube consistent with the conservation of energy, momentum, and atomic species. Because of the rapid reactions (3) through (9) listed below, the densities of OH(v = 0) and OH(v = 1) were steady state.

$$\text{OH}(v = 0): \quad O + OH(0) \longrightarrow O_2 + H \qquad (3)$$

$$H_2 + OH(0) \longrightarrow H_2O + H \qquad (4)$$

$$N + OH(0) \longrightarrow NO + H \qquad (5)$$



Preceding Page BLANK

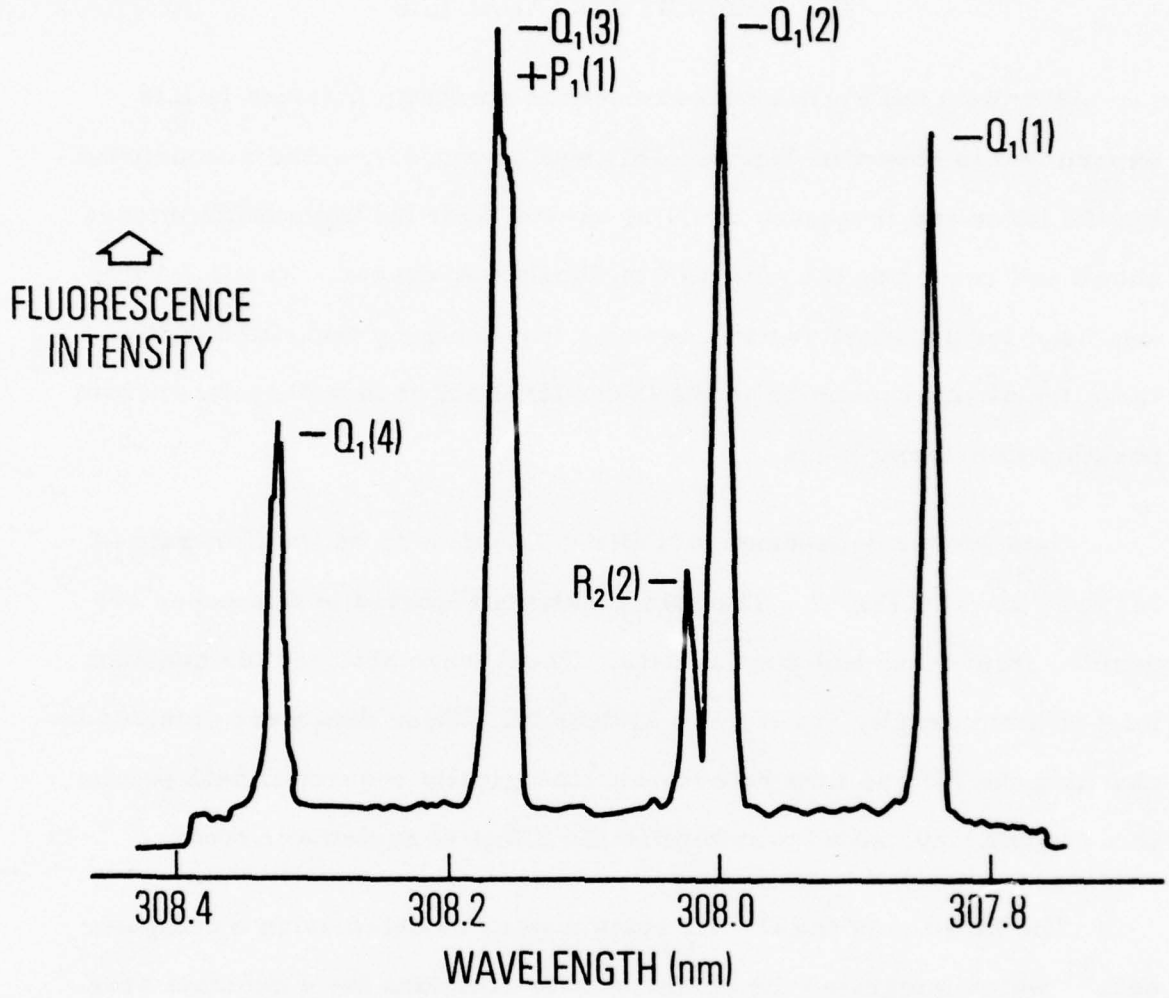


Fig. 6. An Excitation Fluorescence Spectrum of the (0-0) Band in OH. The OH was generated by reaction in the O + $H_2$ system. The lines are identified according to the nomenclature of Ref. 14.

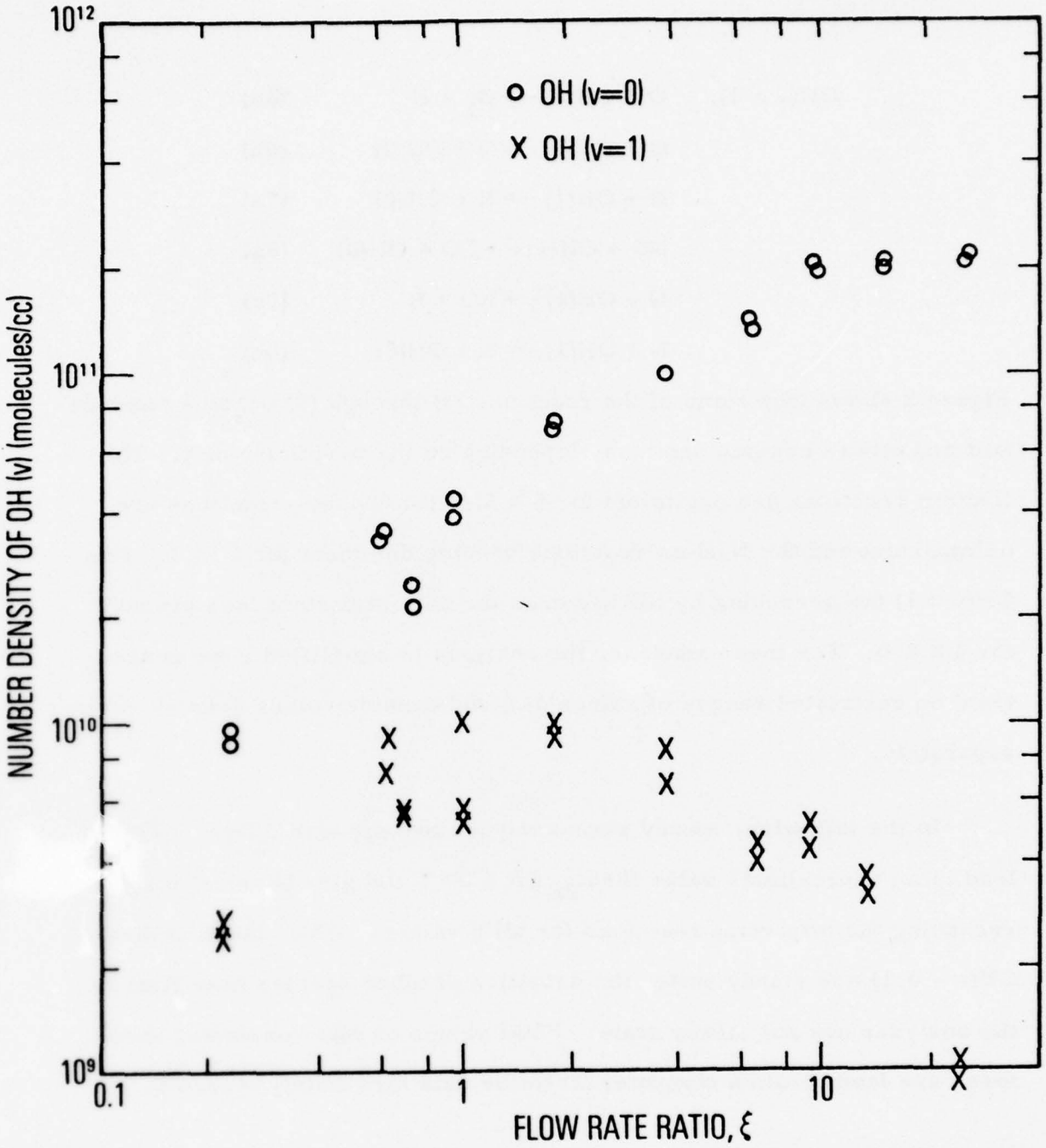


Fig. 7. Data for the Density of OH(v = 0, 1) As a Function of the Flow Rate of NO for Constant N-Atom Flow Rate

$$\text{OH}(v = 1): \quad \text{O} + \text{OH}(1) \longrightarrow \text{O}_2 + \text{H} \qquad (6a)$$

$$\text{O} + \text{OH}(1) \longrightarrow \text{O} + \text{OH}(0) \qquad (6b)$$

$$\text{H} + \text{OH}(1) \longrightarrow \text{H} + \text{OH}(0) \qquad (7a)$$

$$\text{NO} + \text{OH}(1) \longrightarrow \text{NO} + \text{OH}(0) \qquad (8a)$$

$$\text{N} + \text{OH}(1) \longrightarrow \text{NO} + \text{H} \qquad (9a)$$

$$\text{N} + \text{OH}(1) \longrightarrow \text{N} + \text{OH}(0) \qquad (9b)$$

Figure 2 shows why some of the reactions (3) through (9) become unimportant and others become dominant depending on the magnitude of $\xi$. The N-atom reactions are negligible for $\xi \geq 1.0$; the O-atom reactions are unimportant and the N-atom reactions become dominant for $\xi \ll 1$. For OH(v = 1) the quenching by NO becomes the only important loss process for $\xi \geq 8.0$. For these reasons, the analysis is simplified if we concentrate on restricted ranges of values of $\xi$ and consider other $\xi$-value regions separately.

In the following, steady state analyses are presented first. These lead to an approximate value for $k_{2a}$ for $\xi \gg 1$ and give physical insight regarding the important reactions for all $\xi$ values. While the densities of OH(v = 0, 1) are steady state, the densities of other species important in the analyses are not steady state. Final values of rate constants, therefore, are found from a computer fit to the data for [OH(v)] versus $\xi$.

a. $\xi \gg 1$

Analysis of the computer calculations shows that the complete steady state expressions for $\xi \gg 1$ are:

$$[OH(v = 1)] =$$

$$\frac{k_{2a}[O][H_2(1)] + k_{10b}[H][NO_2] + k_{11b}[O][HNO] + [OH(2)]\left(k_{8b}[NO] + k_{7b}[H]\right)}{k_{8a}[NO]} \quad (e)$$

and,

$$[OH(v = 0)] =$$

$$\frac{k_{2b}[O][H_2(1)] + k_{10a}[H][NO_2] + k_{11a}[O][HNO] + [OH(1)]\left(k_{8a}[NO] + k_{7a}[H] + k_{6b}[O]\right)}{k_3[O] + k_4[H_2(0)]} \quad (f)$$

where,

$$H + OH(2) \longrightarrow H + OH(1) \qquad (7b)$$

$$NO + OH(2) \longrightarrow NO + OH(1) \qquad (8b)$$

$$H + NO_2 \longrightarrow OH(v) + NO \qquad (10)$$

and 10a, 10b, 10c, 10d refer to the formation of $OH(v = 0, 1, 2, 3)$, respectively, and

$$O + HNO \longrightarrow OH(0) + NO \qquad (11a)$$

$$O + HNO \longrightarrow OH(1) + NO \qquad (11b)$$

The $NO_2$ in reaction (10) is formed from the reaction

$$O + NO + M \longrightarrow NO_2 + M \qquad (12)$$

The HNO in reaction (11) is formed in

$$H + NO + M \longrightarrow HNO + M \qquad (13)$$

Thus, both $NO_2$ and HNO are present in significant quantities only for $\xi \gg 1$. The OH(2) appearing in expression (e) comes from reaction (10).

Of the terms in the numerator of expression (e), the first one involving $k_{2a}$ has the largest value. The second term involving reaction (10b) is of comparable magnitude only for $\xi > 25$. The third and fourth terms are smaller still. Thus, to first approximation we can ignore the second, third and fourth terms to arrive at an approximate expression for $k_{2a}$.

$$k_{2a} \approx \frac{k_{8a}[NO][OH(v = 1)]}{[O][H_2(v = 1)]} \qquad (g)$$

Glass[13] has recently obtained a value for $k_{8a}$. The densities of $H_2(v = 1)$ and $OH(v = 1)$ are available from the experiment and the densities of O and NO can be calculated accurately from the measured NO flow rates at $\xi = 1$ and at the condition for which $[OH(v = 1)]$ is measured.

A corresponding simplification of expression (f) to arrive at an expression for $k_{2b}$ is not possible. This occurs because for a good match between experimental data and computed values for $[OH(0)]$, the value of $k_{2b}$ must be made so small as to be negligible in comparison with the sum of the other terms in the numerator of expression (f). Furthermore, there is no region in the range of $\xi$-values ($\xi \gg 1$) where one of the remaining terms in the numerator of (f) is clearly dominant. Thus, a simple expression is not obtainable from which any one of the rates $k_{2b}$, $k_{10a}$, $k_{8a}$, $k_{7a}$, or $k_{6b}$ could be deduced in terms of the reasonably well known values[5] for $k_3$ and $k_4$, and the density of OH(0). However, since values are available in the literature for $k_{10}$,[28, 29, 30] $k_{10a}$,[13, 17] $k_{8a}$,[13] $k_{7a}$,[13] and $k_{6b}$,[31] an upper limit to $k_{2b}$ can be established.

The data from which a value of $k_{2a}$ was deduced, by means of expression (g) are given in Table II. From these we find $\overline{k_{2a}} \simeq 1.8 \times 10^{-14}$ cc/molecule-sec using the value of $k_{8a}$ from Ref. 13. This is an approximate value; a more accurate value is obtained from the computer simulation which accounts for the processes in expression (e) which were neglected in deriving expression (g).

Table II. Experimental Data Used to Find $(k_{2a}/k_{8a})$ from Expression (g)

| ξ | [NO][a] | [O] | [$H_2$(v = 1)] | [OH(v = 1)] | $k_{2a}/k_{8a}$ |
|---|---|---|---|---|---|
| 6.5 | 2.08(14)[b] | 2.41(13) | 1.93(14) | 2.96(9) | 1.32(-4) |
| 6.5 | 2.08(14) | 2.41(13) | 1.93(14) | 2.65(9) | 1.19(-4) |
| 9.3 | 3.13(14) | 2.11(13) | 1.93(14) | 3.34(9) | 2.57(-4) |
| 9.3 | 3.13(14) | 2.11(13) | 1.93(14) | 2.88(9) | 2.21(-4) |
| 11.8 | 7.05(14) | 2.74(13) | 1.93(14) | 2.55(9) | 3.40(-4) |
| 11.8 | 7.05(14) | 2.74(13) | 1.93(14) | 1.57(9) | 2.09(-4) |
| 13.5 | 4.75(14) | 1.87(13) | 1.93(14) | 2.43(9) | 3.20(-4) |
| 13.5 | 4.75(14) | 1.87(13) | 1.93(14) | 2.12(9) | 2.79(-4) |
| 17.6 | 1.08(15) | 1.93(13) | 1.99(14) | 1.18(9) | 3.32(-4) |
| 17.6 | 1.08(15) | 1.93(13) | 1.99(14) | 1.18(9) | 3.32(-4) |
| 24.0 | 8.73(14) | 1.39(13) | 1.93(14) | 6.90(8) | 2.25(-4) |
| 24.0 | 8.73(14) | 1.39(13) | 1.93(14) | 6.37(8) | 2.07(-4) |

Average value: $\overline{(k_{2a}/k_{8a})} = (2.48 \pm .76) \times 10^{-4}$

[a]Densities are expressed in molecules/cc.

[b]By definition: 2.08(14) ≡ $2.08 \times 10^{14}$ in this table.

b. $\xi \approx 1$

The steady state expressions in this region are:

$$[OH(1)] = \frac{k_{2a}[O][H_2(1)]}{[O](k_{6a} + k_{6b}) + [H]k_{7a} + [H_2(0)](k_{14a} + k_{14b})} \quad (h)$$

and

$$[OH(0)] = \frac{[O]\left(k_1[H_2(0)] + k_{2b}[H_2(1)]\right) + [OH(1)]\left(k_{6b}[O] + k_{7a}[H] + k_{14b}[H_2]\right)}{k_3[O] + k_4[H_2(0)]} \quad (i)$$

where,

$$H_2(0) + OH(1) \longrightarrow H_2O + H \quad (14a)$$

$$H_2(0) + OH(1) \longrightarrow H_2(1) + OH(0) \quad (14b)$$

Expression (h) shows that there is only one source of OH(v = 1), i.e., reaction (2a), but now there are several important loss processes, no one of which is clearly dominant. The reactions (14a) and (14b) for which Spencer et al.[32] have determined upper limits only, are not as important as reactions (6) and (7a). The H-atoms are produced mostly by reaction (2) with minor contributions from (3) and (4), and we have no experimental measurement of [H]. This makes the determination of a rate constant a nonlinear problem which is best handled by the computer simulation.

With regard to OH(0), the situation is qualitatively as stated previously for $\xi \gg 1$. In order to match the data, the value of $k_{2b}$ must be

so small as to make reaction (2b) a negligible source of OH(0). The major sources of OH(0) are now the physical deactivation of OH(1) by H and O. It is true, though, that the total deactivation rate of OH(v = 1) is smaller for $\xi \approx 1$ than it is for $\xi \gg 1$. This is because the NO density is greatly reduced (see Fig. 2) while the densities of the other major deactivating species stay approximately the same. This means that an experimentally derived upper limit to $k_{2b}$ is best determined from data where $\xi \approx 1$, since for all other conditions reaction 2b is a correspondingly smaller fraction of the total rate of formation of OH(0).

### c. $\xi \ll 1$

In this region it is found that the unknown rate constants for processes (9a) and (9b) must play an important role. Therefore, it is not possible to learn anything further regarding the reactions of interest by analyzing data in this region. However, using the values for $k_{2a}$ and $k_{2b}$ determined for $\xi \geq 1$ it is possible to deduce values for $k_{9a}$ and $k_{9b}$ from the data for $\xi < 1$. This is to be the subject of another paper to be published in the near future.[33]

### d. Final Rate Constants

Extensive computer calculations were carried out to determine the best values for $k_{2a}$ and the upper limit to $k_{2b}$. The value of $k_{2a}$, which brings calculated and measured values of [OH(1)] into agreement, was

determined for all data for which $\xi \geq 1$. This includes more data than are shown in Table II. The average of these values was $\bar{k}_{2a} = (1.0 \pm 0.4) \times 10^{-14}$ cc/molecule-sec. The uncertainty is an experimental uncertainty and represents one standard deviation. The computed densities of OH(v = 0, 1) for this value of $k_{2a}$ are shown in Fig. 7 as the solid lines. For this calculation the value of $k_{2b}$ was set to zero. The values used for all other important rates in this computation are listed in Appendix B.

With $k_{2a} = 1.0 \times 10^{-14}$, computations were done for a range of values of $k_{2b}$. These were done with the values of rate constants for other reactions which affect [OH(0)] chosen to minimize their contribution to [OH(0)], consistent with forming an upper limit to $k_{2b}$. The value of $k_{2b}$ which brought about agreement between calculated and measured [OH(0)] was determined for each data point in the range $0.9 \leq \xi \leq 2.0$. The average value was $\bar{k}_{2b} \leq 4.7 \times 10^{-15}$ cc/molecule-sec. This must be taken as an upper limit to the true value since Fig. 7 shows that computations with $k_{2b} = 0.0$ give a reasonably good fit to the data.

### e. Sensitivity Analysis

The values of the rate constants reported here are, of course, sensitive to uncertainties in the rates of certain other reactions as used in the computer simulations.

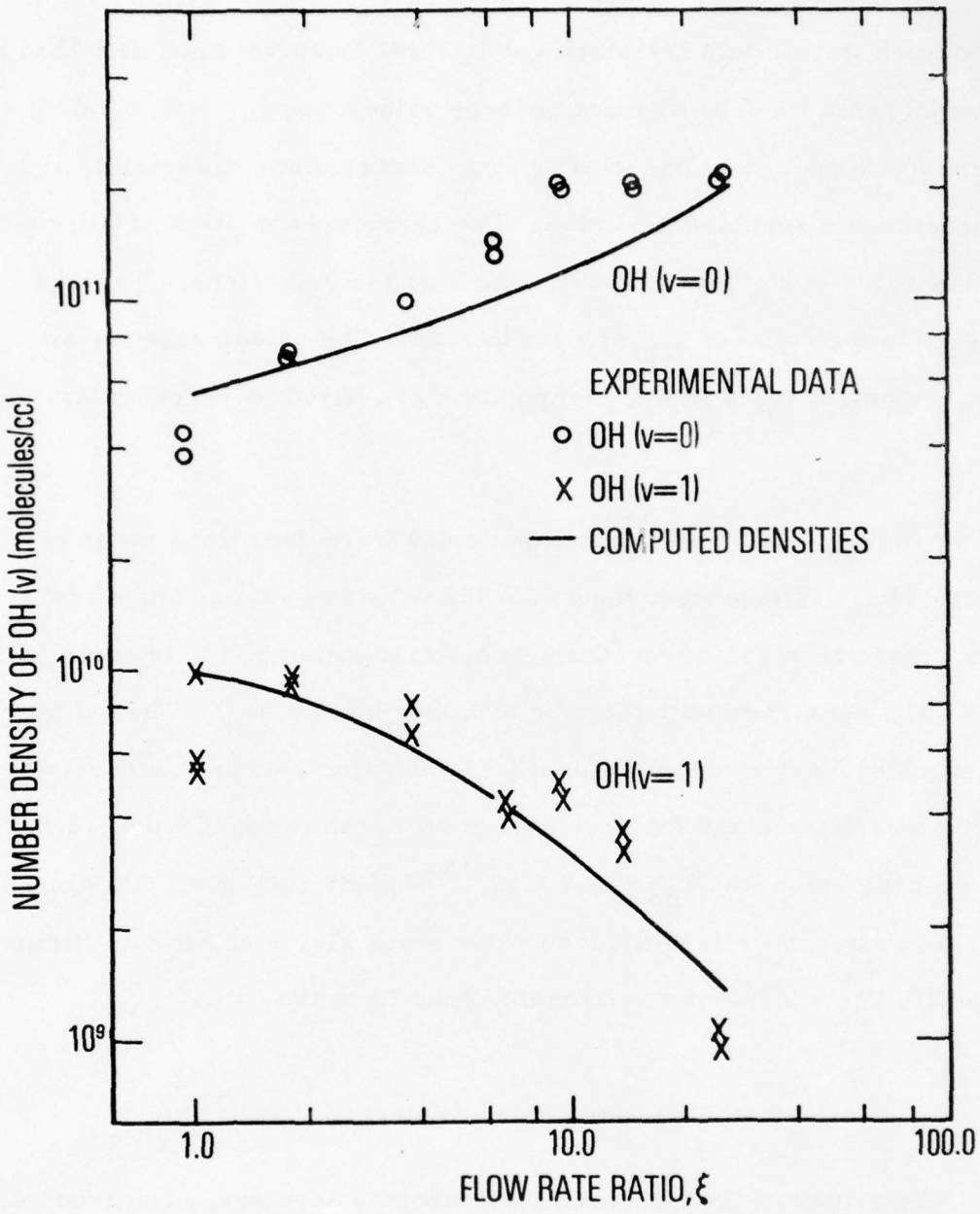


Fig. 8. Comparison of the Computer-Calculated Densities of OH(v = 0, 1) With the Experimental Data Shown in Fig. 7. For this calculation, $k_{2a} = 1.0 \times 10^{-14}$ cc/molecule-sec and $k_{2b} = 0.0$.

The most important sources of OH(v) in these experiments other than reactions (2) are the following reaction sequences:

$$O + NO + M \longrightarrow NO_2 + M \qquad (12)$$

followed by

$$H + NO_2 \longrightarrow OH(v \leq 3) + NO \qquad (10)$$

and

$$H + NO + M \longrightarrow HNO + M \qquad (13)$$

followed by

$$O + HNO \longrightarrow OH(v \leq 5) + NO \qquad (11)$$

Experimentally measured values of reaction rate have been reported for all of these except reaction (11). There has been extensive recent work on each of the other three reactions. These three were also reviewed by Baulch et al.[5,34] Baulch's suggested uncertainty in reaction (12) is ± 20% and measurements have been reported for M = $N_2$ and M = $H_2$, the principal constituents in the experiments reported here. The overall reaction rate for reaction (10) has been the subject of three recent studies.[28,29,30] These three yield values for $k_{10}$ which are in substantial agreement with one another but which differ by a factor of about 2.5 from the previously held value.[34] It seems certain that the more recent values are to be preferred. When the data from Refs. 28 29, and 30 are weighted equally the value, $k_{10} = (1.22 \pm .08) \times 10^{-10}$ is obtained[28] for T = 298°K. It is also true that the vibrational branching ratios for reaction (10), although they have recently received much attention,[13,16,17] are still not accurately known. Spencer and Glass[13] have used Bemand's value[29] $k_{10} = 1.1 \times 10^{-10}$ in interpreting their measurements of the quenching rates for

$$NO + OH(v) \longrightarrow NO + OH(v - 1) \quad (8)$$

$$H + OH(v) \longrightarrow H + OH(v - 1) \quad (7)$$

Spencer and Glass have presented their data for these rates in such a way that new values can be derived for different values of the overall rate and branching ratios of reaction (10). We have reinterpreted Spencer and Glass's results for the rates of (7) and (8) for $k_{10} = 4.8 \times 10^{-11}$ cc/molecule-sec and for a set of vibrational branching ratios consistent with the work of Silver et al.[17] and Polanyi and Sloan.[16] The relative rates are 1.0/1.3/1.3/0.13 for v = 0 to 3, respectively. In assessing the overall uncertainty in $k_{2a}$, the values $k_{10} = 1.3 \times 10^{-10}$, the ratios $k_{10a}/k_{10b}/k_{10c}/k_{10d}$ = 1.0/1.3/1.3/0.13, respectively and Spencer's reported values for $k_7$ and $k_8$ were used in determining a lower limit, while $k_{10} = 4.8 \times 10^{-11}$, $k_{10a}/k_{10b}/k_{10c}/k_{10d}$ = 1.0/0.7/0.3/0.03 and appropriately modified values of $k_7$ and $k_8$ were used in determining an upper limit.

Baulch et al.[34] suggest an uncertainty of ± 50% for the rate of (13) with M = $H_2$. No values seem to have been reported for M = $N_2$. We shall assume that the rate for M = $N_2$ is the same as for M = $H_2$ for purposes of this uncertainty analysis.

While a lower limit has been placed[35] on $k_{11}$ ($\geq 1.8 \times 10^{-11}$), nothing is known about the branching ratios for forming OH(v). With $k_{11} = 1.8 \times 10^{-11}$, then reaction (13) is rate limiting and larger values of $k_{11}$ will have no effect on the calculated OH density.

For our purposes then, it is quite sufficient to assume that $k_{11a} = 0.0$ and $k_{11b} = 1.8 \times 10^{-11}$ cc/molecule-sec., i.e., that only OH(v = 1) is formed when a lower limit to $k_{2a}$ is being evaluated; conversely we assume that $k_{11a} = k_{11b} = 0$ when an upper limit is being evaluated.

One other issue needs to be addressed with regard to these possibly interfering reactions (10) through (13). H-atoms are formed by thermal dissociation of $H_2$ on the hot tungsten filament. They also are formed by the reactions of interest,

$$O + H_2 \longrightarrow OH + H.$$

If one calculates the equilibrium dissociation level at the measured temperature of the tungsten filament one finds that the H-atom flow rate contributed by the filament is roughly comparable to that formed by subsequent reaction after the reactants are mixed. This means that uncertainties in the density of H-atoms assumed to be coming from the filament might be important in determining the best value for $k_{2a}$, since [H] enters the picture through both reactions (10) and (13) as well as reaction (7). Attempts were made early in this project to infer the H-atom flow rate from the filament in separate experiments. These consisted of allowing the hydrogen coming from the hot filament to mix with a stream of $N_2$ carrying a known amount of $NO_2$ gas. The products of reaction were examined for

OH molecules by laser induced fluorescence. The absolute density of OH(0) was used in conjunction with the known $NO_2$ flow rate to infer an initial H-atom density. The result of these measurements was that the inferred value of [H] was at, or slightly below the equilibrium value over the filament temperature range from 800°C to 1150°C.

Accordingly, the simulation calculations were performed with an H-atom flow rate determined by equilibrium dissociation at the filament temperature.

Computer calculations were carried out in which the rates of all important reactions were allowed to vary over the ranges indicated in Appendix B. The process of determining a value for $k_{2a}$ for each data point was repeated to find upper and lower limits to $\bar{k}_{2a}$ consistent with these rate constant uncertainties. The results of this analysis are: $\bar{k}_{2a} = (1.0 \, {}^{+\,0.3}_{-\,0.6}) \times 10^{-14}$ cc/molecule-sec. It is seen that the experimental uncertainty of $(\pm\, 0.4) \times 10^{-14}$ is not greatly different from the uncertainty arising from uncertain rate constants. Thus, our best estimate of $k_{2a}$ is:

$$\bar{k}_{2a} = (1.0 \, {}^{+\,0.4}_{-\,0.6}) \times 10^{-14} \text{ cc/molecule-sec.}$$

With regard to the upper limit to $k_{2b}$, the values for the rates of competing reactions were already set to their respective uncertainty limits for the computations described in Section d. Hence, the reported upper limit to $k_{2b}$ takes into consideration these other uncertainties.

The reported value for $k_{2a}$ and upper limit to $k_{2b}$ can be summed to obtain the total reaction rate of $O(^3P)$ with $H_2(v = 1)$. Thus,

$$\bar{k}_2 = \bar{k}_{2a} + \bar{k}_{2b} = (1.0 \,^{+0.9}_{-0.6}) \times 10^{-14} \text{ cc/molecule-sec.}$$

## IV. DISCUSSION

The question naturally arises whether there might be contributions to the observed reaction rate from vibrational levels in $H_2$ higher than $v = 1$. Vibrationally excited $H_2$ is generated by a thermal source in this experiment and there is every reason to expect that higher vibrational states are represented in the flow. The $H_2$ vibrational temperature implied by measured values of $[H_2(v = 1)]$ is $T_V \approx 1100^\circ K$. Even if the original source were not thermal there would be a rapid redistribution of vibrational energy by nearly resonant V-V exchange between $H_2$ molecules.

While it cannot be rigorously proven that higher vibrational levels ($v \geq 2$) are not contributing to the observed OH production, the following strongly inferential observation has been made. Data were obtained for the dependence of $OH(v \leq 1)$ on the density of $H_2(v = 1)$. These data will be the subject of a future publication. *If $H_2(v \geq 2)$ were significant* the dependence of $[OH(v)]$ on $[H_2(1)]$ would be expected to be of order larger than one. In fact, the data show that $[OH(v)]$ is of order one or less in $[H_2(1)]$. Thus, it is felt that $H_2(v \geq 2)$ does not contribute to the observed $OH(v)$ and that the measured rate constant refers strictly to $H_2(v = 1)$ reactant.

The largest possible value of $\bar{k}_2$ consistent with the uncertainties determined above is $(\bar{k}_2)_{max} = 1.9 \times 10^{-14}$. This is smaller by a comfortable margin than the upper limit,

$$k_2 \leq 1 \times 10^{-13} \text{ cc/molecule-sec.}$$

previously reported by Birely et al.[6]

Preceding Page BLANK

The reported value represents an increase owing to vibrational excitation in hydrogen by a factor of $\approx 2.6 \times 10^3$ over the rate of reaction (1), although the rate of reaction (1) has never been measured at $T \approx 300^\circ K$. The acceleration of a reaction process by vibrational energy in one of the reactants is characterized by some authors[36] by the fraction, $\alpha$, of the vibrational quantum, $E_{VIB}$, which is effective in reducing the activation energy for that reaction. From this approach the ratio $k^\ddagger/k$ of vibrationally accelerated rate to ground state rate constants is

$$k^\ddagger/k = \exp(\alpha E_{VIB}/RT).$$

For the value of $k_2$ reported herein, it is found that $\alpha \approx 0.43$.

There are two classical trajectory treatments of reaction (2) in the literature with different approaches. Johnson and Winter[8] did a collinear OHH analysis using an LEPS potential surface. The barrier height was first adjusted to bring about agreement between the calculated and measured[5,4] rate constants for the fully ground state reaction. Whitlock et al.[9] generated a diatomics-in-molecules potential surface which confirmed that collinear hydrogen abstraction was the dominant $O(^3P) + H_2$ reaction path. Johnson and Winter report an expression for the rate constant for reaction (2) of $k_2 = 4.65T \times 10^{-14} \exp(-1868/T)$. At room temperature this gives $k_2 = 2.9 \times 10^{-14}$, a value in remarkably good agreement with the experimental value reported herein. Whitlock et al. report a range of values for $k_2$ of $1.9 \times 10^{-13} \leq k_2 \leq 8.3 \times 10^{-13}$ at $T = 300^\circ K$. Johnson and Winter also report an expression for the branching ratio, $\Gamma \equiv k_{2a}/k_{2b}$ of $\Gamma = 2.3 \exp(196/T)$. This leads to a value of $k_{2a} = 2.27 \times 10^{-14}$, again in

reasonably good agreement with experiment. The theoretically determined value for $k_{2b}$, i.e., $k_{2b} = 5.15 \times 10^{-15}$ at room temperature is very close to the experimental upper limit of $k_{2b} \leq 4.7 \times 10^{-15}$ cc/molecule-sec.

The good agreement between the result of Johnson and Winter and the present experimental result does not necessarily attest to the accuracy of their potential surface because of the uncertainties introduced by a classical treatment of vibrations and because tunneling is not modeled. The results of Ref. 9 confirm the predominance of the collinear abstraction mode but give a considerably different predicted rate constant.

The present understanding of the effect of vibrational energy on the reaction of O-atoms with $H_2$ is summarized graphically in Fig. 9. It is seen that the theoretical expression for $k_2$ from Ref. 8 lies slightly above the uncertainty range of the experimental measurement reported herein.

It is of interest to examine the implications of the rate of reaction (2) for the measurement of the rate of reaction (1) at high temperatures. At sufficiently high temperatures, assuming thermal equilibrium between translational and vibrational modes, there will be enough $H_2(v = 1)$ present to affect the apparent rate of reaction (1). Indeed, recent measurements[2] of $k_1$ at high temperatures($1400^\circ K \leq T \leq 1900^\circ K$) give values which are significantly larger than predicted by a simple Arrhenius expression which fits all of the data in the temperature range $900 \geq T \geq 400^\circ K$. The possibility that this upward curvature at high temperatures might be the result of reaction (2) was suggested by Gardiner.[37] It should be pointed

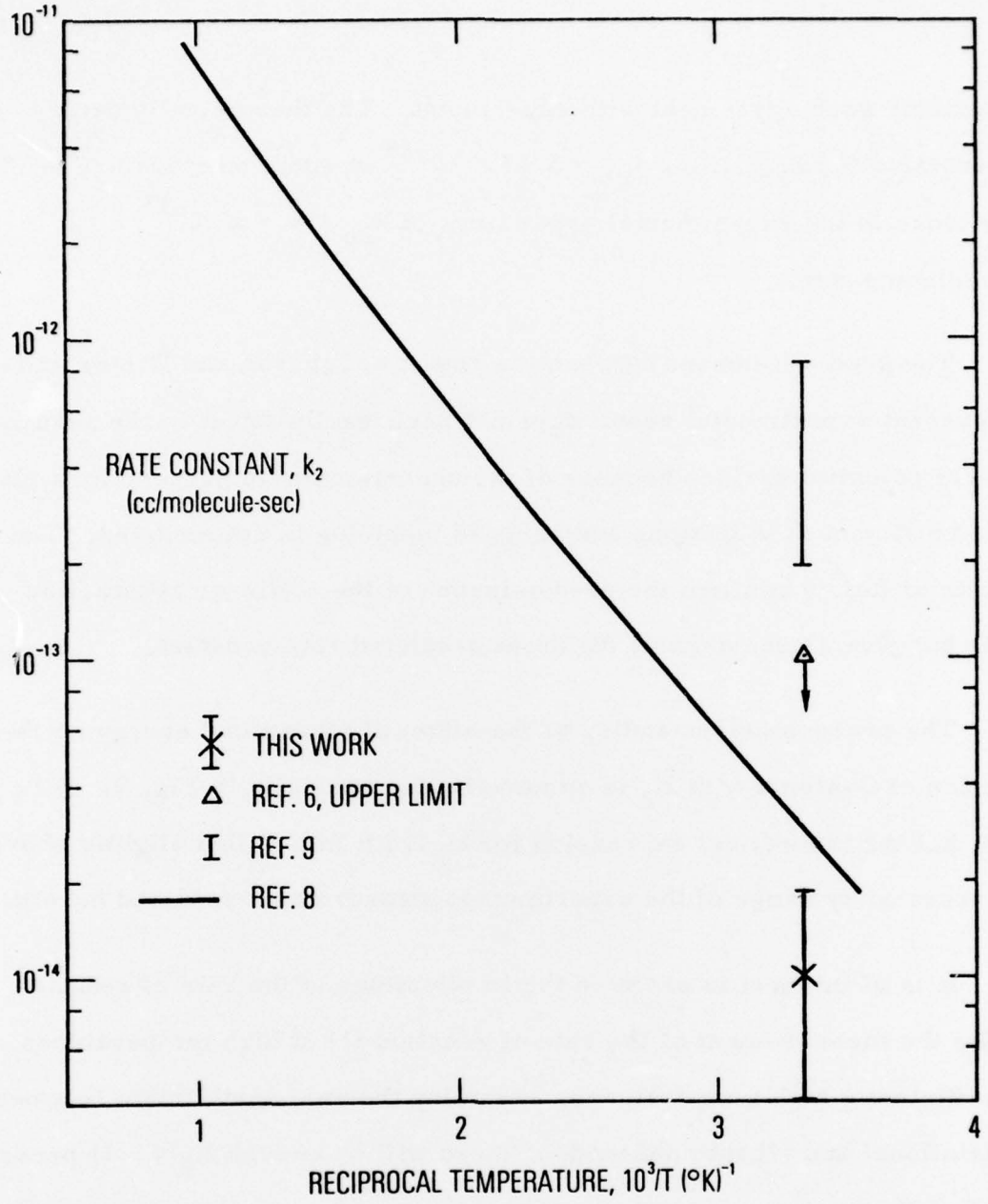


Fig. 9. A Summary of Present Knowledge of the Rate Constant for Reaction (2). The figure includes the upper limit reported in Ref. 6, the measured value reported in this work, and the results of the two theoretical treatments of Refs. 8 and 9.

out here that non-Arrhenius behavior is not a particularly surprising result even for a fully ground state reaction. It is the purpose of this exercise to establish only whether or not the vibrationally accelerated reaction might be responsible for the observed curvature.

We adopt the Arrhenius expression given by Johnson and Winter for $k_2$, which is in good agreement with our experimental result at T = 302°K, and calculate the total rate of reaction $k_t$, including the effect of $H_2(v = 1)$ according to the following expression:

$$k_t = \frac{k_1[H_2(v = 0)] + k_2[H_2(v = 1)]}{\sum_v [H_2(v)]} \qquad (j)$$

For $k_1$ we adopt the consensus expression presented by Baulch et al.[5] The result is shown in Fig. 10 along with the data of Schott et al.,[2] the results of a transition state theory(t. s. t.)-BEBO calculation also presented by Schott, and the Baulch expression for $k_1$. It is seen that $k_t$, according to expression (j) above, does not match the data of Schott et al. as well as do the t. s. t. calculations. The differences are small, however, and a final resolution must await data for the value of $k_2$ in the temperature range T ~ 2000°K.

The observation, reported herein for the first time, of the existence of vibrational excitation in $H_2$ when $H_2$ is mixed with active nitrogen may have implications for previous measurements for T < 400°K of the fully ground state reaction rate constant, i.e., reaction (1). There have been at least three reports[1, 3, 4] of the value of this rate constant for which the unknown existence of vibrationally excited hydrogen produced by energy

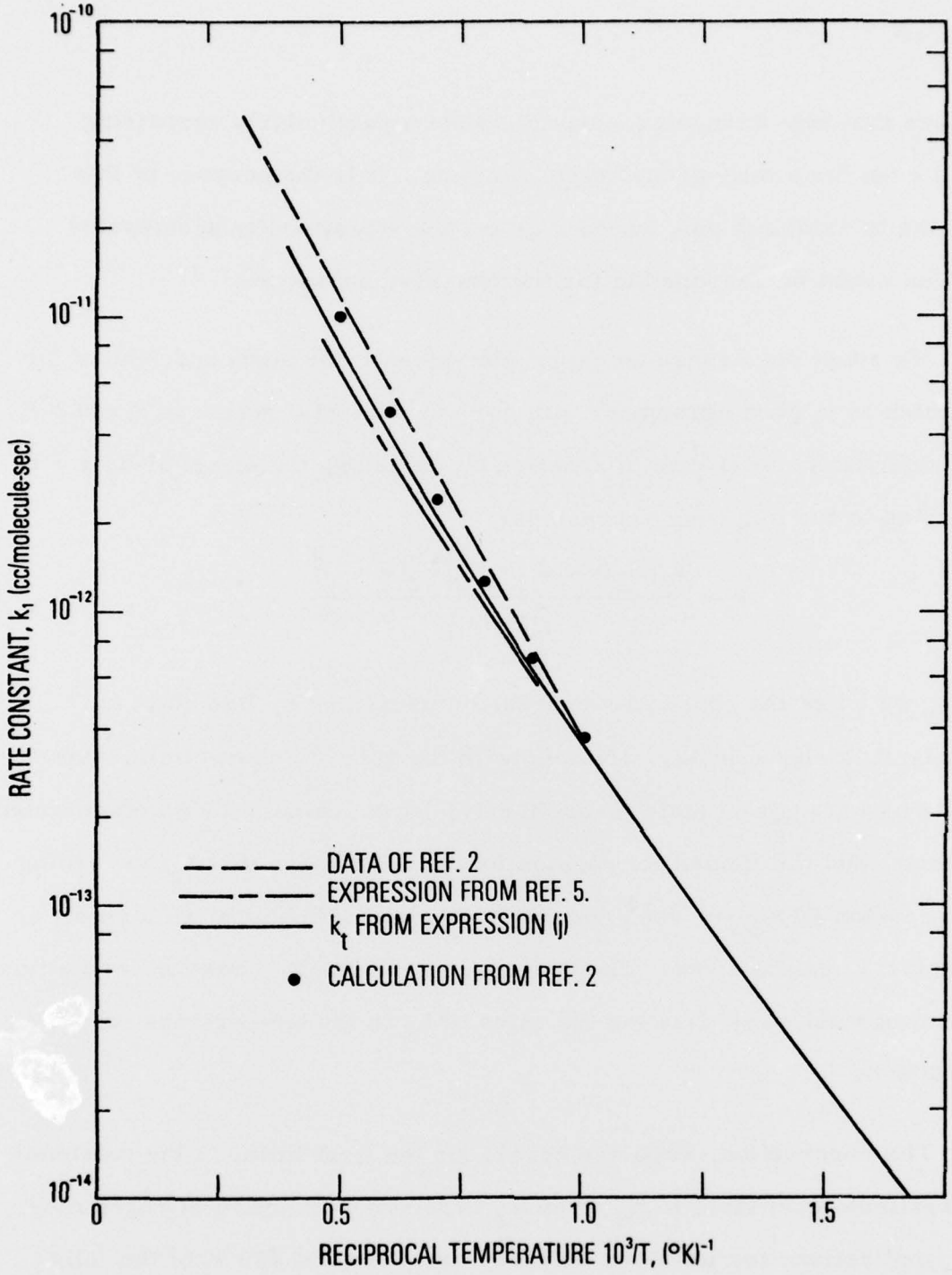


**Fig. 10. The Rate Constant for Reaction (1) in the High Temperature Region**

exchange from active $N_2$ could have been a factor. Among these three reports there are significant differences in the reported rate constant values at low temperatures where the effect of undetected vibrationally excited $H_2$ would be most pronounced. We have obtained measurements for the rate of reaction (1) at a lower temperature than previously reported by any investigators. These measurements were obtained with careful monitoring and accounting for the effects of possible $H_2(v = 1)$. These results will be reported separately.[38]

## REFERENCES


[1] R. N. Dubinsky and D. J. McKenney, Can. J. Chem. 53, 3531 (1975).

[2] G. L. Schott, R. W. Getzinger and W. A. Seitz, Int. J. Chem. Kin. VI, 921 (1974).

[3] A. A. Westenberg and N. DeHaas, J. Chem. Phys. 50, 2512 (1969).

[4] I. M. Campbell and B. A. Thrush, Trans. Far. Soc. 64, 1265 (1968).

[5] D. L. Baulch, D. D. Drysdale, D. G. Horne and A. C. Lloyd, "Evaluated Kinetic Data for High Temperature Reactions," (Butterworth and Co., London, 1972), Vol. 1, p. 49.

[6] J. H. Birely, J. V. V. Kasper, F. Hai and L. A. Darnton, Chem. Phys. Lett. 31, 220 (1975).

[7] The upper limit to $\alpha$ for this reaction was erroneously reported in Ref. 6 as $\alpha \leq 0.30$. The value should have read $\alpha \leq 0.53$, to be consistent with the upper limit to $k_2$ which was correctly reported as $k_2 \leq 1.0 \times 10^{-13}$ cc/molecule-sec.

[8] B. R. Johnson and N. W. Winter, J. Chem. Phys. 66, 4116 (1977).

[9] P. A. Whitlock, J. T. Muckerman and E. R. Fisher, "Theoretical Investigations of the Energetics and Dynamics of the Reactions $O(^3P, {}^1D) + H_2$ and $C(^1D) + H_2$," Ph.D. Thesis of P. A. Whitlock, Wayne State University, Detroit, Michigan, November 1976.


Preceding Page BLANK - Fi

[10]Curves of growth for several transitions in the $H_2$ Lyman system have been published in, J. H. Birely, S. J. Young, L. A. Darnton, F. Hai, J. V. V. Kasper, Report No. TR-0075(5270-20)-2, 31 December 1974, The Aerospace Corporation, El Segundo, California.

[11]G. A. Takacs and G. P. Glass, J. Phys. Chem. 77, 1060 (1973).

[12]F. Kaufman, J. Chem. Phys. 28, 992 (1958).

[13]J. E. Spencer and G. P. Glass, Chem. Phys. 15, 35 (1976).

[14]G. H. Dieke and H. M. Crosswhite, J. Quant. Spect. Rad. Transfer 2, 97 (1962).

[15]G. C. Light and J. H. Matsumoto, to be published.

[16]J. C. Polanyi and J. J. Sloan, Int. J. Chem. Kin., Spec. Symposium, September 1975.

[17]J. A. Silver, W. L. Dimpfl, J. H. Brophy and J. L. Kinsey, J. Chem. Phys. 65, 1811 (1976).

[18]K. R. German, J. Chem. Phys. 64, 4065 (1976).

[19]N. Omenetto, P. Benetti, L. P. Hart, J. D. Winefordner, C. Th. J. Alkemade, Spectrochim. Acta 28B, 289 (1973).

[20]N. Omenetto, L. P. Hart, P. Benetti, J. D. Winefordner, Spectrochim. Acta 28B, 301 (1973).

[21]E. H. Piepmeier, Spectrochim. Acta 27B, 431 (1972).

[22]E. H. Piepmeier, Spectrochim. Acta 27B, 445 (1972).

[23]D. K. Killinger, C. C. Wang and M. Hanabusa, Phys. Rev. A 13, 2145 (1976).

[24]R. K. Lengel and D. R. Crosley, Chem. Phys. Lett. 32, 261 (1975).

[25]D. R. Crosley and R. K. Lengel, J. Quant. Spect. Rad. Transfer 15, 579 (1975).

[26]P. E. Rouse and R. Engleman, Jr., J. Quant. Spect. Rad. Transfer 13, 1503 (1973).

[27]E. B. Turner, G. Emanuel, R. L. Wilkins, Report No. TR-0059 (6240-20)-1, Vol. 1, 30 July 1970, The Aerospace Corporation, El Segundo, California.

[28]M. A. A. Clyne and P. B. Monkhouse, J. Chem. Soc. Faraday II, 73, 298 (1977).

[29]P. P. Bemand and M. A. A. Clyne, Part 6, J. Chem. Soc. Faraday II, 73, 394 (1977).

[30]H. G. Wagner, D. Welzbacher and R. Zellner, Ber. Bunsenges. Phys. Chem. 80, 1023 (1976).

[31]J. E. Spencer and G. P. Glass, Int. J. Chem. Kin. 9, 97 (1977).

[32]J. E. Spencer, H. Endo and G. P. Glass, Proceedings of 16th Symposium (International) on Combustion, Cambridge, Mass., 15-20 Aug 1976, p. 829.

[33]G. C. Light, to be published.

[34]D. L. Baulch, D. D. Drysdale, D. G. Horne and A. C. Lloyd, "Evaluated Kinetic Data for High Temperature Reactions," (Butterworth and Co., London, 1973) Vol. 2.

[35]I. M. Campbell, B. J. Handy, J. Chem. Soc. Far. Trans. I, 71, 2097, (1975).

[36]J. H. Birely and J. L. Lyman, J. Photochem. 4, 269 (1975).

[37]W. C. Gardiner, Jr., W. G. Mallard, M. McFarland, K. Morinaga, J. H. Owen, W. T. Rawlins, T. Takeyama, B. F. Walker, 14th Symposium (international) on Combustion, (The Combustion Institute, Pittsburgh, Pennsylvania, 1973), p. 61.

[38]G. C. Light, to be published.

[39]The author will gladly supply interested parties with the specifications of reactions which were used but do not appear in Appendix B.

## Appendix A

### Reactions Used for the Calculation of Species Concentrations in the N + NO System

Included here are the specifications and rate coefficients for all of the chemical reactions used to calculate species concentrations resulting from the titration of active nitrogen with NO. The rate coefficients are represented by three coefficients a, b, c such that the rate constant k is given by

$$k = aT^{b}\exp(c/T),\ \text{cc/mole-sec}$$

where T is in degrees Kelvin. The numbering of the reactions is different from that used in the text.

| Reaction | a | b | c |
|---|---|---|---|
| (1) $N + NO \longrightarrow N_2 + O$ | $3.1 \times 10^{13}$ | 0 | -168. |
| (2) $2O + M \longrightarrow O_2 + M$ | $1.4 \times 10^{18}$ | -1.0 | -171. |
| (3) $O + O_2 + M \longrightarrow O_3 + M$ | $1.7 \times 10^{13}$ | 0 | +1057. |
| (4) $O + NO + M \longrightarrow NO_2 + M$ | $1.05 \times 10^{15}$ | 0 | +941. |
| (5) $O + N + M \longrightarrow NO + M$ | $6.4 \times 10^{16}$ | -0.5 | 0 |
| (6) $2N + M \longrightarrow N_2 + M$ | $2.8 \times 10^{14}$ | 0 | +503. |
| (7) $O + O_3 \longrightarrow 2O_2$ | $1.2 \times 10^{13}$ | 0 | -2416. |
| (8) $N + O_2 \longrightarrow NO + O$ | $6.4 \times 10^{9}$ | +1.0 | -3145. |
| (9) $O + NO_2 \longrightarrow O_2 + NO$ | $1.0 \times 10^{13}$ | 0 | -302. |
| (10) $O + NO \longrightarrow NO_2 (+ h\nu)$ | $3.4 \times 10^{12}$ | -2.0 | 0 |
| (11) $NO + O_3 \longrightarrow NO_2 + O_2$ | $5.7 \times 10^{11}$ | 0 | -1309. |
| (12) $N + NO_2 \longrightarrow N_2O + O$ | $9.03 \times 10^{11}$ | 0 | 0 |

In addition, the removal of O at the wall was simulated by specifying a first order rate constant, $k_w = -3.4\ sec^{-1}$, for use in the expression:

$$\left(\frac{\partial[O]}{\partial t}\right)_{wall} = k_w[O]$$

## Appendix B

### Reactions Used for Computer Calculations in the $O + H_2$ System

Assembled here are the 20 most important chemical reactions and rate coefficients used in the computer analyses described in the text for the $O + H_2$ system. A total of 102 reactions were used in each of the computations but only 20 of these proved to be important. Only those reactions which significantly affected the concentration of any species are included in the following list. In particular, many reactions involving the production and destruction of $HO_2$, $H_2O_2$, $HNO_2$, $HNO_3$, and $N_2O$ were used in the computation but do not appear below[39] because none of them were significant for calculated concentrations of OH(0, 1). The nomenclature is the same as used in Appendix A but the numbering of the reactions is the same as that used in the text.

| Reaction | a | b | c | Uncertainty |
|---|---|---|---|---|
| (1) $O + H_2(0) \longrightarrow OH(0) + H$ | $1.8 \times 10^{10}$ | +1.0 | -4480. | - |
| (3) $O + OH(0) \longrightarrow O_2 + H$ | $2.3 \times 10^{13}$ | 0 | 0 | ±30% |
| (4) $H_2(0) + OH(0) \longrightarrow H_2O + H$ | $2.2 \times 10^{13}$ | 0 | -2590. | ±20% |
| (5) $N + OH(0) \longrightarrow NO + H$ | $3.2 \times 10^{13}$ | 0 | 0 | - |
| (6a) $O + OH(1) \longrightarrow O_2 + H$ | $6.32 \times 10^{13}$ | 0 | 0 | ±50% |
| (6b) $O + OH(1) \longrightarrow O + OH(0)$ | $8.73 \times 10^{13}$ | 0 | 0 | ±20% |
| (7a) $H + OH(1) \longrightarrow H + OH(0)$ | $1.63 \times 10^{14}$ | 0 | 0 | +0% -56% |
| (7b) $H + OH(2) \longrightarrow H + OH(1)$ | $1.99 \times 10^{14}$ | 0 | 0 | +9% -56% |

| | Reaction | a | b | c | Uncertainty |
|---|---|---|---|---|---|
| (8a) | $NO + OH(1) \rightarrow NO + OH(0)$ | $4.52 \times 10^{13}$ | 0 | 0 | +0%<br>-56% |
| (8b) | $NO + OH(2) \rightarrow NO + OH(1)$ | $7.23 \times 10^{13}$ | 0 | 0 | +9%<br>-56% |
| (10a) | $H + NO_2 \rightarrow OH(0) + NO$ | $3.71 \times 10^{13}$ | 0 | 0 | +6%<br>-80% |
| (10b) | $H + NO_2 \rightarrow OH(1) + NO$ | $2.59 \times 10^{13}$ | 0 | 0 | +6%<br>-60% |
| (10c) | $H + NO_2 \rightarrow OH(2) + NO$ | $1.04 \times 10^{13}$ | 0 | 0 | +6%<br>-60% |
| (11a) | $O + HNO \rightarrow NO + OH(0)$ | $6.0 \times 10^{12}$ | 0 | 0 | +0%<br>-100% |
| (11b) | $O + HNO \rightarrow NO + OH(1)$ | $6.0 \times 10^{12}$ | 0 | 0 | +0%<br>-100% |
| (12a) | $O + NO + N_2 \rightarrow NO_2 + N_2$ | $1.54 \times 10^{15}$ | 0 | +940. | ±20% |
| (12b) | $O + NO + H_2 \rightarrow NO_2 + H_2$ | $1.82 \times 10^{15}$ | 0 | +940. | ±20% |
| (13) | $H + NO + M \rightarrow HNO + M$ | $5.4 \times 10^{15}$ | 0 | +300. | ±50% |
| (14a) | $H_2(0) + OH(1) \rightarrow H_2O + H$ | $6.0 \times 10^{9}$ | 0 | 0 | +0%<br>-30% |
| (14b) | $H_2(0) + OH(1) \rightarrow H_2(1) + OH(0)$ | $6.0 \times 10^{9}$ | 0 | 0 | +0%<br>-100% |

In addition, removal at the wall was handled by assigning the following first order rate constants:

| Species | $k_w$, $sec^{-1}$ |
|---|---|
| O | -3.4 |
| H | -4.0 |
| $H_2(1)$ | -46.0 |
| OH(0) | -30.0 |
| OH(1) | -80.0 |

## THE IVAN A. GETTING LABORATORIES

The Laboratory Operations of The Aerospace Corporation is conducting experimental and theoretical investigations necessary for the evaluation and application of scientific advances to new military concepts and systems. Versatility and flexibility have been developed to a high degree by the laboratory personnel in dealing with the many problems encountered in the nation's rapidly developing space and missile systems. Expertise in the latest scientific developments is vital to the accomplishment of tasks related to these problems. The laboratories that contribute to this research are:

Aerophysics Laboratory: Launch and reentry aerodynamics, heat transfer, reentry physics, chemical kinetics, structural mechanics, flight dynamics, atmospheric pollution, and high-power gas lasers.

Chemistry and Physics Laboratory: Atmospheric reactions and atmospheric optics, chemical reactions in polluted atmospheres, chemical reactions of excited species in rocket plumes, chemical thermodynamics, plasma and laser-induced reactions, laser chemistry, propulsion chemistry, space vacuum and radiation effects on materials, lubrication and surface phenomena, photosensitive materials and sensors, high precision laser ranging, and the application of physics and chemistry to problems of law enforcement and biomedicine.

Electronics Research Laboratory: Electromagnetic theory, devices, and propagation phenomena, including plasma electromagnetics; quantum electronics, lasers, and electro-optics; communication sciences, applied electronics, semiconducting, superconducting, and crystal device physics, optical and acoustical imaging; atmospheric pollution; millimeter wave and far-infrared technology.

Materials Sciences Laboratory: Development of new materials; metal matrix composites and new forms of carbon; test and evaluation of graphite and ceramics in reentry; spacecraft materials and electronic components in nuclear weapons environment; application of fracture mechanics to stress corrosion and fatigue-induced fractures in structural metals.

Space Sciences Laboratory: Atmospheric and ionospheric physics, radiation from the atmosphere, density and composition of the atmosphere, aurorae and airglow; magnetospheric physics, cosmic rays, generation and propagation of plasma waves in the magnetosphere; solar physics, studies of solar magnetic fields; space astronomy, x-ray astronomy; the effects of nuclear explosions, magnetic storms, and solar activity on the earth's atmosphere, ionosphere, and magnetosphere; the effects of optical, electromagnetic, and particulate radiations in space on space systems.

*THE AEROSPACE CORPORATION*
El Segundo, California

• • •

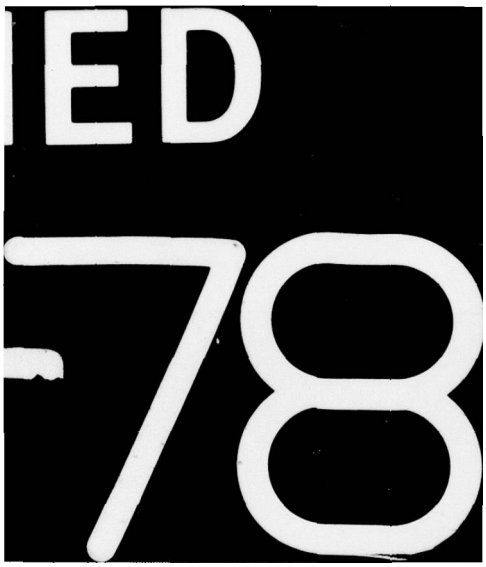
ED
78